PERFORMANCE OF LAP SPLICES IN CONCRETE MASONRY SHEAR WALLS

By

JON ZACHERY MJELDE

A thesis submitted in partial fulfillment of
the requirements for the degree of

MASTER IN SCIENCE IN CIVIL ENGINEERING

WASHINGTON STATE UNIVERSITY
Department of Civil and Environmental Engineering

APRIL 2008

To the Faculty of Washington State University:

The members of the Committee appointed to examine the thesis of JON ZACHERY MJELDE find it satisfactory and recommend that it be accepted.

_____
Chair

_____

_____

ACKNOWLEDGEMENTS

The financial support provided by the National Concrete Masonry Association Education and Research Foundation, the Northwest Concrete Masonry Association, and the Masonry Industry Promotion Group of Spokane, Washington is gratefully acknowledged. I would also like to acknowledge the support of the Bob Fraser Masonry Graduate Fellowship at Washington State University.

I offer my deepest thanks to Dr. David McLean for inviting me to graduate school, seeing that I attend a professional conference in Australia, serving as chair of my committee, and providing constant guidance and support throughout this project.

I thank Dr. Mohamed Elgawady and Dr. David Pollock for serving on my committee. I also thank Tim Thompson, Steve Knappers and Dave Fangione of the Bricklayers and Allied Craftworkers Local No. 3 for constructing the masonry walls used in this study. I am grateful for the assistance provided by Courtney Davis, Bob Duncan, Scott Lewis, Mesay Endeshaw, Garth Nelson, Valentine Amar, and Fred Barker during the construction and testing phases of this research.

Finally, I thank my family and Gretchen Dole for their ongoing support.

PERFORMANCE OF LAP SPLICES IN CONCRETE

MASONRY SHEAR WALLS

Abstract

by Jon Zachery Mjelde, M.S.
Washington State University
April 2008

Committee Chair: David I. McLean

This research investigated the performance of reinforcement lap splices in concrete masonry shear walls detailed and loaded to represent more realistic conditions. Nine concrete masonry shear walls incorporating flexural reinforcement lap splices at the bases of the walls were constructed and subjected to in-plane cyclic loading. Additionally, nine concrete masonry panels incorporating identical lap splices were constructed and subjected to direct tension. There appear to be no significant differences in the performance of a lap splice tested in direct tension and in-plane flexure. This finding supports the validity of the large amount of data and resulting code design equation based on direct tension loading of lap splices.

Results from the lap splice tests of this study confirm that reduced masonry cover significantly affects lap performance, supporting the need to address cover for lap splice design. Walls containing No. 6 (M#19) bars offset in the cells performed poorly with respect to ultimate load resistance, displacement capacity, and peak longitudinal reinforcement stresses compared to walls with similar amounts of reinforcement distributed in the center of the cells, even when provided with lap lengths of 60 bar diameters.

For the parameters considered in this study, the current MSJC requirements predicted the performance of lap splices for No. 6 (M#19) bars centered and offset in the cells with

reasonable accuracy. However, the provisions appear to be overly conservative for lap splices of No. 8 (M#25) bars by roughly 20%; this may be a result of confinement provided by transverse reinforcement in the walls. These results also suggest that perhaps little or no benefit was provided by the transverse reinforcement for walls containing No. 6 (M#19) bars.

TABLE OF CONTENTS

Page

ACKNOWLEDGEMENTS iii

ABSTRACT iv

LIST OF FIGURES ix

LIST OF TABLES xi

CHAPTERS

1. CHAPTER 1: INTRODUCTION 1

1.1. Background 1

1.2. Scope and Objectives 1

2. CHAPTER 2: LITERATURE REVIEW 3

2.1. Introduction 3

2.2. Historic Design Equation (Simplified Equation) 3

2.3. Previous Lap Splice Research 4

2.4. 2005 MSJC Lap Splice Equation 5

2.5. 2006 IBC Splice Provisions 6

2.6. NCMA Lap Splice Research 7

2.6.1. Phase 1 - MR26 7

2.6.2. Phase 2 – MR27 7

2.6.3. Phase 3 – MR32 8

3. CHAPTER 3: EXPERIMENTAL PROGRAM 10

3.1. Introduction 10

3.2. Phase I – Walls 10

3.2.1. Description of Footings.....10

3.2.2. Description of Wall Specimens 11

3.2.3. Material Properties for Wall Specimens 14

3.2.4. Wall Specimen Construction 16

3.2.5. Test Setup for Wall Specimens.....17

3.2.6. Instrumentation for Wall Specimens 19

3.2.7. System Control and Data Acquisition.....19

3.2.8. Test Procedures for Wall Specimens 20

3.3. Phase II – Panels.....21

3.3.1. Description of Panel Specimens 21

3.3.2. Material Properties for Panel Specimens.....22

3.3.3. Panel Specimen Construction 24

3.3.4. Test Setup for Panel Specimens.....25

3.3.5. System Control, Data Acquisition, and Test Procedures.....26

4. CHAPTER 4: RESULTS OF WALL TESTS 27

4.1. Introduction.....27

4.2. Phase I – Results of Wall Testing.....27

4.2.1. Typical Ultimate Failure Mechanism 27

4.2.2. Wall 1 - No. 8 (M#25) bars, 48 d_b 28

4.2.3. Wall 5 - No. 6 (M#19) bars distributed, 48 d_b 30

4.2.4. Wall 7 - No. 6 (M#19) bars offset, 48 d_b 32

4.2.5. Reinforcement Stresses at Failure in Wall Specimens 34

4.2.6. Backbone Curves 36

4.3. Phase II – Results of Panel Testing 39

4.3.1. Typical Ultimate Failure Mechanism 39

4.3.2. Testing Irregularities.....40

4.3.3. Panel 9 - No. 6 (M#19) bars offset, 60 d_b 40

4.3.4. Reinforcement Stresses at Failure in Panel Specimens 41

4.4. Conclusions.....42

5. CHAPTER 5: ANALYSIS OF TEST RESULTS 44

5.1. Introduction.....44

5.2. Comparison of Testing Methods 44

5.3. Comparisons with Simplified Equation.....46

5.4. Comparisons with Current MSJC Equation 47

5.5. Confinement Effects of Different Transverse Reinforcement Details 49

6. CHAPTER 6: CONCLUSIONS 50

6.1. Summary.....50

6.2. Conclusions.....50

REFERENCES 53

APPENDIX.....55

LIST OF FIGURES

Page

Figure 3.1. Reinforcement Configuration: Walls 1, 2, 3 & 4; No. 8 (M#25) Bars.....11

Figure 3.2. Reinforcement Configuration: Walls 5 & 6; No. 6 (M#19) Bars Distributed.11

Figure 3.3. Reinforcement Configuration: Walls 7, 8 & 9; No. 6 (M#19) Bars Offset.....11

Figure 3.4. Provided Horizontal Reinforcement - Walls 1, 2 & 4 - No. 4 (M#13) Bar.....13

Figure 3.5. Provided Horizontal Reinforcement - Wall 3 - Two No. 3 (M#10) Bars.....13

Figure 3.6. Provided Horizontal Reinforcement - Walls 5 & 6 - No. 4 (M#13) Bar.....13

Figure 3.7. Provided Horizontal Reinforcement - Walls 7, 8 & 9 - No. 4 (M#13) Bar.....13

Figure 3.8. Typical Wall Specimen 14

Figure 3.9. Installation of Loading Bolts.....17

Figure 3.10. Testing Setup - Walls 18

Figure 3.11. Data Acquisition Flow Chart (adapted from Snook, 2005).....20

Figure 3.12. Displacement-based Loading Protocol.....21

Figure 3.13. Typical Panel Specimen 22

Figure 3.14. Testing Setup - Panels 26

Figure 4.1. Cracking and Lap Failures - Wall 1 29

Figure 4.2. Hairline Radial Crack - Wall 1 29

Figure 4.3. Load-Displacement Hysteresis Curves; Wall 1.....30

Figure 4.4. Cracking and Lap Failure - Wall 5 31

Figure 4.5. Load-Displacement Hysteresis Curves - Wall 5 32

Figure 4.6. Cracking and Lap Failure - Wall 7 33

Figure 4.7. Load-Displacement Hysteresis Curves - Wall 7 34

Figure 4.8. Backbone Curves - Walls 1-4 37

Figure 4.9. Backbone Curves - Walls 5-6 38

Figure 4.10. Backbone Curves - 7-9 39

Figure 4.11. Cracking and Lap Failure; Panel 9 41

Figure 5.1. Provided % of 48 d_b versus σ_{Test}/F_y - Walls & Panels 46

Figure 5.2. Provided % of Req. MSJC Lap Length versus σ_{Test}/F_y - Walls & Panels 48

LIST OF TABLES

Page

Table 3.1. Provided Laps and Side Cover - Walls 12

Table 3.2. Compressive Material Strengths - Walls 15

Table 3.3. Tension Yield Strengths.....16

Table 3.4. Compressive Material Strengths - Panels 23

Table 3.5. Provided Laps - Panels 24

Table 4.1. Ratios of Developed Stress and Specified Yield Stress - Walls 36

Table 4.2. Ratios of Developed Stress and Specified Yield Stress - Panels 42

Table 5.1. Comparison of Developed Stresses 45

Table 5.2. Values where Extensions of Best-Fit Lines Cross Axes – Walls & Panels.....49

CHAPTER 1: INTRODUCTION

1.1 Background

Splices of reinforcing bars are required for the construction of most masonry structures. While various splicing methods exist, including proprietary mechanical devices, lap splices of the bars are the most widely-used and cost-effective method. The current lap splice provisions in the 2005 Masonry Standards Joint Committee (MSJC) *Building Code Requirements for Masonry Structures* are largely based on research performed in the late 1990's. Since the introduction of these provisions, there has been considerable discussion about the validity of the provisions, in part because they can produce very large and impractical lap lengths when certain parameters are encountered.

The 2005 provisions are well supported by laboratory tests of lap splices. Most of the tests upon which the provisions are based, however, involved loading the lap splices in direct tension, and the test panels typically did not contain any reinforcement transverse to the lapped bars. While this loading scheme provides a clear indication of lap performance, it does not represent typical loading of lap splices in real structures. Additionally, recent research from the National Concrete Masonry Association (2005) has shown improvements in lap splice behavior resulting from confinement to the lap splice from horizontal reinforcement.

1.2 Scope and Objectives

The primary objective of this research was to evaluate the behavior of reinforcement lap splices in concrete masonry shear walls detailed and loaded to represent more realistic conditions. Variables investigated in this study include length of lap, size of bar, concentrated

versus distributed reinforcement, reduced cover resulting from bars offset in the cells, and method of testing. Nine concrete masonry shear walls incorporating flexural reinforcement lap splices at the bases of the walls were constructed and subjected to in-plane cyclic loading. Additionally, nine concrete masonry panels incorporating identical lap splices were constructed and subjected to direct tension.

CHAPTER 2: LITERATURE REVIEW

2.1 Introduction

In this chapter, previous research and design equations related to lap splices are presented and discussed. Several iterations preceded the 2005 MSJC lap splice design equation, and discovering its evolution is helpful for understanding the context of this research.

2.2 Historic Design Equation (Simplified Equation)

In the 2005 edition of the MSJC Code, a single equation is provided for lap splice design. However, in previous editions of the MSJC, separate lap splice equations existed for Allowable Stress Design (ASD) and Strength Design (SD) provisions. The ASD design equation appeared in the MSJC between 1988 and 2005 and is given as Equation 2.1a. An equivalent equation using SI units is presented here as Equation 2.1b.

$$l_s = 0.002 d_b F_s \qquad \text{(Equation 2.1a)}$$

$$l_s = 0.29 d_b F_s \qquad \text{(Equation 2.1b)}$$

where:

l_d = required lap length, in. (mm);

d_b = bar diameter, in.^{2} (mm^2); and

F_s = maximum allowable stress, ksi (MPa)

This equation has a prescriptive minimum splice length of 12 in. (305 mm) to prevent bond failure and pullout.

Although this simple equation is no longer present in the MSJC, it appeared in other building codes for a number of decades preceding the 1988 MSJC, and it is therefore widely

known in the masonry design community. For Grade 60 steel, F_s = 24,000 psi (165.5 MPa), and Equation 2.1 simplifies to $l_s = 48d_b$. While this simplified equation is easy to apply, testing showed that it is unconservative for large bar sizes and small masonry cover. This simplified equation also does not recognize several important parameters known to influence lap splice performance, including the strength of masonry assemblage, effects of reduced masonry cover, and effects of possible confinement from horizontal reinforcement across the bars being developed.

2.3 Previous Lap Splice Research

Extensive lap splice research was completed in the last two decades. Major contributors to this research included: Soric and Tulin from the University of Colorado at Boulder (Soric 1987); The US Army Corps of Engineers in association with Atkinson-Noland & Associates (Hammons 1994); Thompson from Washington State University (Thompson 1998); and the Council for Masonry Research (CMR 1998); and the National Concrete Masonry Association (NCMA 2004, 2005, 2007). Collectively, this research embodies a wide range of specimen variables, including: 8 in. (203 mm) and 12 in. (305 mm) concrete masonry panels; 4 in. (102 mm) and 6 in. (152 mm) clay masonry panels; bar sizes from No. 4 (M#13) to No. 11 (M#36); masonry compressive strengths from 1700 psi (11.72 MPa) to 6400 psi (44.13 MPa); varying positions of lap within the panels; and widely varying lap lengths.

This research illustrated, among other things, that as the diameter of reinforcement increases or the cover of masonry decreases, the potential for longitudinal splitting of the masonry assemblage is amplified. The data from this research has had extensive analyses that

will not be repeated here. A new equation was derived to fit this broad set of test data of lap splices loaded in direct tension. An iteration of this equation is presented in the 2005 MSJC.

2.4 2005 MSJC Lap Splice Equation

The design equation for lap splices in the 2005 MSJC is given as Equation 2.2a. An equivalent equation using SI units is presented here as equation 2.2b.

$$l_d = \frac{0.13 d_b^{\,2} f_y \gamma}{K\sqrt{f'_m}} \qquad \text{(Equation 2.2a)}$$

$$l_d = \frac{1.5 d_b^{\,2} f_y \gamma}{K\sqrt{f'_m}} \qquad \text{(Equation 2.2b)}$$

where:

l_d = required lap length, in.(mm);

d_b = bar diameter, in.^{2} (mm^2);

f_y = reinforcement yield strength, psi (MPa);

γ = 1.0 for No.3 through No. 5 bars;

= 1.3 for No. 5 through No. 7 bars;

= 1.5 for No. 8 through No. 9 bars;

K = lesser of [masonry cover, clear spacing of steel, $5d_b$], in. (mm); and

f'_m = strength of masonry assemblage, psi (MPa)

This equation is calibrated to produce 125% of the nominal yield strength of the splice reinforcement, with a prescriptive minimum splice length of 12 in. (305 mm) to prevent bond failure and pullout.

The transition to this equation was based on a desire to include all appropriate variables, not as a response to any recognized lap failures. Although this equation is a good

fit to the data previously mentioned, it has criticisms. One of the primary criticisms of this equation is that it can produce long lap lengths. This criticism was bolstered after some construction problems related to excessive lap lengths were reported. As bar size increases, both γ and d_b increase, resulting in a longer lap length. Also, if masonry cover is reduced, K becomes small and the required lap length increases. Both of these effects can result in significantly longer lap lengths when compared to the $48d_b$ of the simplified equation.

Additionally, questions have been raised over the testing methods used. Most of the tests upon which the equation is based involved loading the lap splices in direct tension. While this loading scheme provides a clear indication of lap performance, it does not represent typical loading of lap splices in real structures. Furthermore, the equation does not recognize the potential beneficial effects of horizontal reinforcement transverse to the lapped bars (NCMA 2004, 2005, 2007).

2.5 2006 IBC Splice Provisions

In the 2006 edition of the International Building Code, separate lap splice equations are presented for Allowable Strength Design (ASD) and Strength Design (SD). The ASD equation is the same as the simplified equation presented earlier (Equation 2.1) except with a prescriptive minimum of 12 in. (305 mm) or 40 bar diameters, whichever is less. The SD equation is the same as the MSJC equation presented earlier (Equation 2.2), except with a prescriptive minimum of 12 in. (305 mm) and a prescriptive maximum of 72 bar diameters.

2.6 NCMA Lap Splice Research

Research from the National Concrete Masonry Association has shown that reinforcement placed transversely to a splice can be effective at providing some degree of confinement and results in significantly improved performance and greater capacity of the splice when tested in direct tension.

2.6.1 Phase 1 - MR26

Fifteen concrete masonry panels were constructed using 8 in. (203 mm) units, consisting of five sets of identical specimens. Two sets of No. 8 (M#25) reinforcing bars were placed in the center of the cells and incorporated a splice length of 48 in. (1219 mm). All specimens were solidly grouted. To evaluate the effects of confinement reinforcement on splice behavior, five different arrangements of lateral reinforcement in the panels were considered. Test results showed that bar reinforcement placed transversely to a splice was effective at providing some degree of confinement and resulted in significantly improved performance and greater capacity of the splice. In the most extreme example, the addition of two No. 4 (M#13) bars placed transversely in each course over the length of a splice resulted in an increase in splice capacity of 50% when compared to a similarly configured splice without lateral confinement.

2.6.2 Phase 2 - MR27

Twenty-seven specimens were constructed using 8-inch (203 mm) concrete masonry units, consisting of nine sets of three identical specimens. All specimens were solidly grouted. In each specimen, a lap splice using No. 6 (M#19) reinforcing bars was placed in the

center of two separate cells, each incorporating a lap splice length of 36 inches (914 mm). To evaluate the effects of confinement reinforcement on splice behavior, nine different arrangements of transverse (horizontal) reinforcement were considered. In all cases, the presence of transverse reinforcement in the form of bed joint reinforcement or horizontal bond beam mild reinforcement noticeably improved splice strength by providing confinement to the splice. In contrast, the presence of confinement hoops appeared to be detrimental to the strength of the splices.

2.6.3 Phase 3 - MR32

Eighty-four wall panels were constructed using 8 inch (203 mm) and 12 inch (305 mm) concrete masonry units. There were 28 total sets of specimens, with three identical panels per set. In each wall panel, one set of lap spliced No. 8 (M#25) reinforcing bars were placed in each of two separate cells. Four lap splice lengths were investigated: 48 inch (1,219 mm), 40 inch (1,016 mm), 32 inch (813 mm), and 24 inch (610 mm). Varying sizes of reinforcing bars were used to provide lateral confinement at the top and bottom of each splice including No. 4 (M#13), No. 6 (M#19), and No. 8 (M#25) bars. Also evaluated for their impact on lap splice performance were No. 3 (M#10) deformed hoops in each course, and a bar positioner in each course. Two sets of specimens were constructed to determine the effects of structural fiber reinforcement in masonry grout. Four sets of panels were constructed using 12 inch (305 mm) masonry units to investigate the effects of positioning of the lateral reinforcement.

The spliced bars confined by the transverse reinforcement were tested in direct tension to determine the strength and performance of the splice. As seen in previous research,

the addition of lateral reinforcement increased the tensile strength of the lap splice. There was very little affect on strength when using the deformed hoops and the bar positioners. With the addition of structural fibers in the grout there was little increase in strength, but the fibers did reduce the amount of cracking on the post fracture surface of the masonry panels.

CHAPTER 3: EXPERIMENTAL PROGRAM

3.1 Introduction

Nine concrete masonry shear walls incorporating flexural reinforcement lap splices at the bases of the walls were constructed and subjected to in-plane cyclic loading. Additionally, nine concrete masonry panels incorporating lap splice details identical to those in the wall specimens were constructed and subjected to direct tension. This chapter provides details of the specimens, testing methods, and data acquisition. It is divided into two sections: Phase I details wall testing and Phase II details panel testing.

3.2 Phase I – Walls

3.2.1 Description of Footings

The wall specimens were constructed on heavily-reinforced concrete footings that anchored the walls to the floor, thus providing rigid support at the wall bases. Footings of the same size and having the same reinforcement were used for all wall specimens. The footings were 68 in. (1727 mm) long, 24 in. (610 mm) wide and 23 in. (584 mm) deep. These were anchored to a laboratory strong floor through eight bolt tubes that were cast into the footing. Footing reinforcement consisted of No. 4 (M#13) shear stirrups at 8 in. (203 mm) on center as well as nine No. 5 (M#16) longitudinal reinforcement bars spaced around the reinforcement cage. Wall flexural reinforcement was anchored into the footing with 90 degree hooks. Four lifting picks comprised of bent No. 3 (M#10) bars were installed on each of the four corners to allow lifting and transport by an overhead crane.

3.2.2 Description of Wall Specimens

The walls were constructed of fully grouted concrete masonry in running bond using standard blocks. All walls were 13 courses high, three blocks wide and had dimensions of 47.6 in. x 7.63 in. x 104 in. (1209 mm x 194 mm x 2642 mm). Three configurations of flexural (vertical) reinforcement were provided in the walls as indicated in Figures 3.1, 3.2, and 3.3.

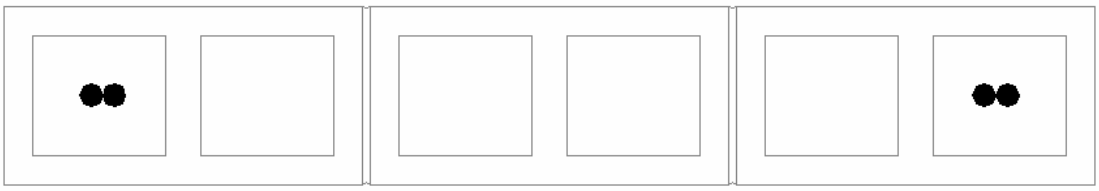

Figure 3.1. Reinforcement Configuration: Walls 1, 2, 3 & 4; No. 8 (M#25) Bars

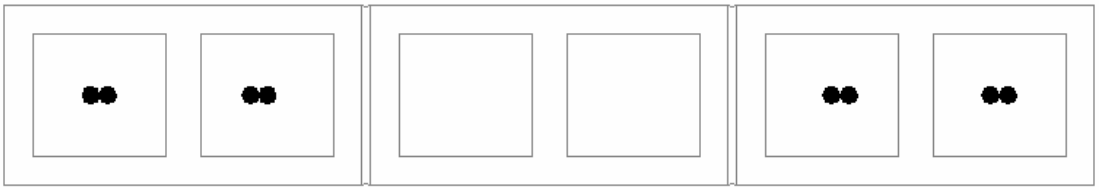

Figure 3.2. Reinforcement Configuration: Walls 5 & 6; No. 6 (M#19) Bars Distributed

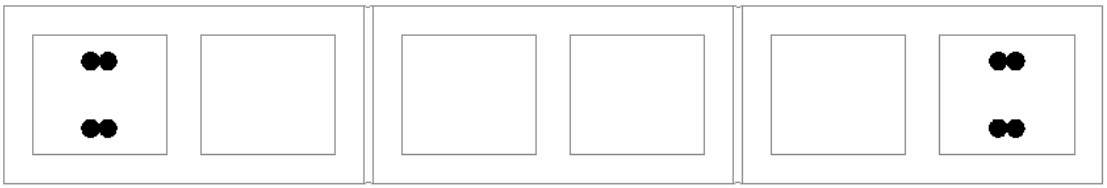

Figure 3.3. Reinforcement Configuration: Walls 7, 8 & 9; No. 6 (M#19) Bars Offset

Varying splice lengths were provided in the walls as indicated in Table 3.1. Values are shown with respect to four measurements: length, bar diameters, percentage of the MSJC equation (Equation 2.2), and percentage of the simplified equation (Equation 2.1). The vertical reinforcement projecting from the footings was discontinued at a height equal to the splice length. Those bars were lapped to bars of equal diameter running the full height of the

wall. Splices were positioned in the walls such that end cover was always greater than or equal to side cover. The MSJC-prescribed minimum cover of 2 in. (51 mm) was used as the side cover in Walls 7,8 and 9. Side cover distances are given in Table 3.1.

Table 3.1. Provided Laps and Side Cover - Walls

Walls	Bar Size	Length, in. (mm)	d_b	% MSJC Equation	% Simplified Equation	Side Cover, in. (mm)
1	No. 8 (M#25)	48 (1219)	48	79%	100%	3.3 (83.8)
2	No. 8 (M#25)	36 (914)	36	59%	75%	3.3 (83.8)
3	No. 8 (M#25)	36 (914)	36	59%	75%	3.3 (83.8)
4	No. 8 (M#25)	60 (1524)	60	99%	125%	3.3 (83.8)
5	No. 6 (M#19)	36 (914)	48	125%	100%	3.4 (86.4)
6	No. 6 (M#19)	27 (686)	36	94%	75%	3.4 (86.4)
7	No. 6 (M#19)	36 (914)	48	74%	100%	2.0 (50.8)
8	No. 6 (M#19)	27 (686)	36	55%	75%	2.0 (50.8)
9	No. 6 (M#19)	45 (1143)	60	92%	125%	2.0 (50.8)

Continuous horizontal reinforcement was provided in all walls such that it exceeded the required shear predicted by moment-curvature analysis. All walls except Wall 3 contained a single No. 4 (M#13) bar in every other course, starting with the first and ending with the last. Wall 3 contained two No. 3 (M#10) bars at every other course, starting with the first and ending with the last. For Walls 1 through 6, the horizontal bars were anchored with 180-degree hooks around the outermost vertical reinforcement. For Walls 7 through 9, the horizontal bars were anchored with 90-degree hooks angled downwards between the two

vertical reinforcing bars. Drawings of the provided horizontal reinforcement are given in Figures 3.4, 3.5, 3.6 and 3.7. A drawing of a typical wall specimen is given in Figure 3.8.

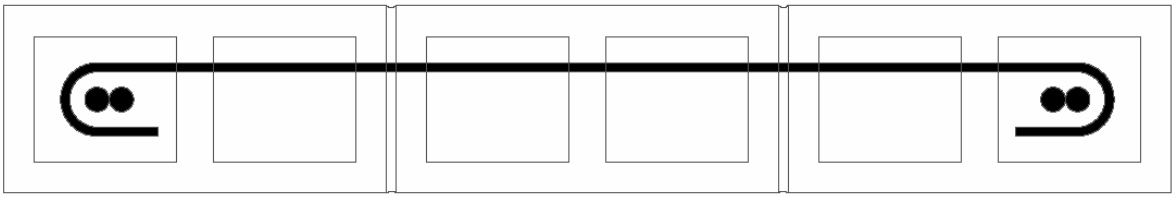

Figure 3.4. Provided Horizontal Reinforcement - Walls 1, 2 & 4 - No. 4 (M#13) Bar

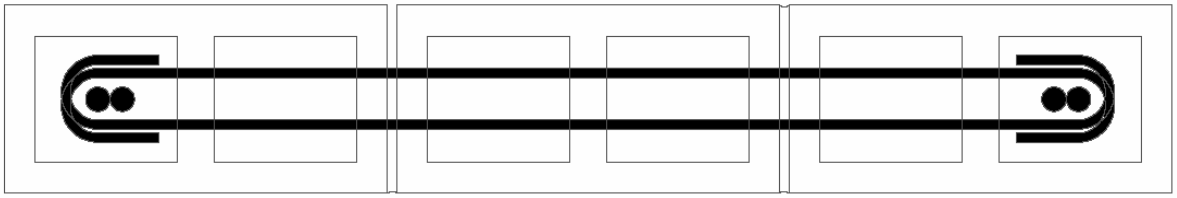

Figure 3.5. Provided Horizontal Reinforcement - Wall 3 - Two No. 3 (M#10) Bars

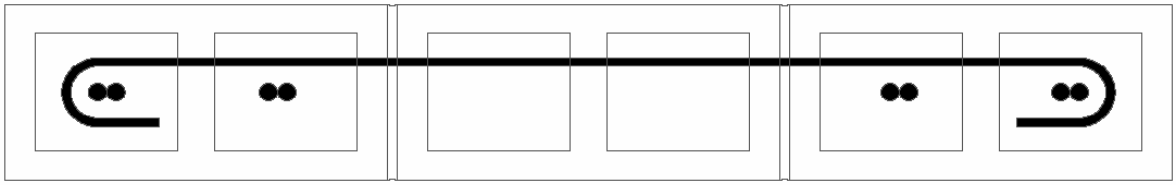

Figure 3.6. Provided Horizontal Reinforcement - Walls 5 & 6 - No. 4 (M#13) Bar

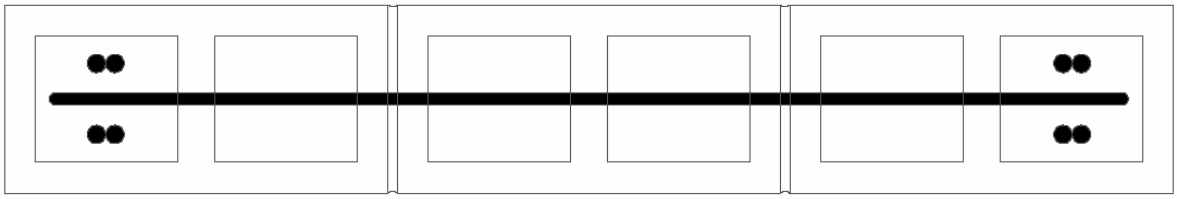

Figure 3.7. Provided Horizontal Reinforcement - Walls 7, 8 & 9 - No. 4 (M#13) Bar

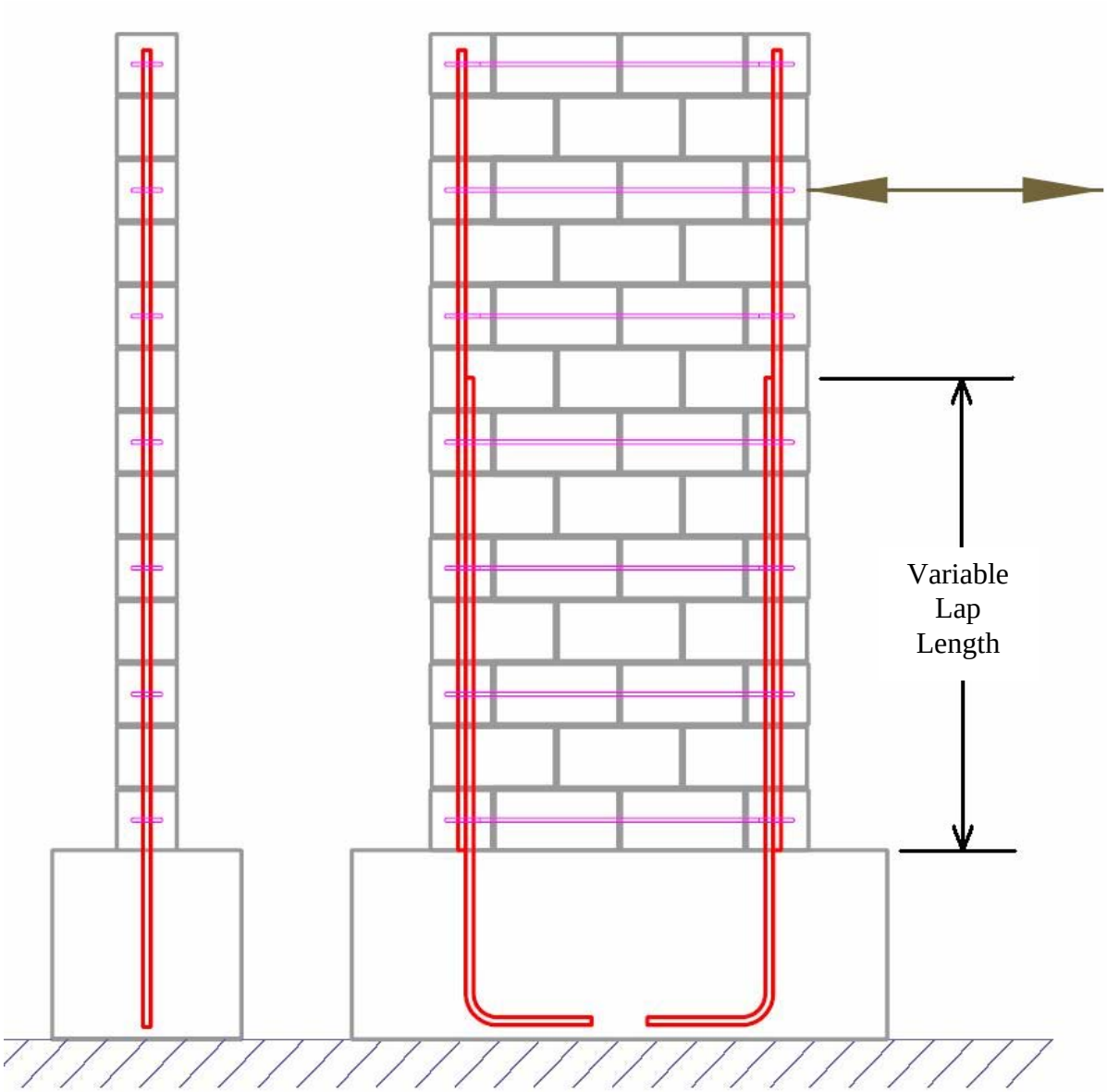

Figure 3.8. Typical Wall Specimen

3.2.3 Material Properties for Wall Specimens

The masonry blocks used for construction were nominally 8 in. x 8 in. x 16 in. (203 mm x 203 mm x 406 mm) hollow concrete masonry units (full) and 8 in. x 8 in. x 8 in. (203 mm x 203 mm x 203 mm) hollow concrete masonry units (half). Three of the blocks were set aside and capped for testing. Full bond-beam units were used in every other course, starting

with the first and ending with the last, to accommodate horizontal shear reinforcement. Standard half blocks and dead-end-bond blocks were used as needed. Type S mortar was mixed onsite and used for construction. Three test cylinders of the mortar (conforming to ASTM C780), 2 in. (51 mm) diameter by 4 in. (102 mm) height, were made during construction and set aside for testing. 7-sack course aggregate grout was used in the wall specimens. The grouting was completed in two separate lifts; three grout prisms (conforming to ASTM C1019), 3.5 in. (89 mm) square x 7 in. (178 mm) high, were made from each mix, set aside and capped for testing. Three block prisms (conforming to ASTM C1314) were made during construction, set aside and capped for testing. These samples were all testing according to ASTM standards, and the average compressive strengths for the materials are given in Table 3.2.

Table 3.2. Compressive Material Strengths - Walls

	Mortar	Grout		Masonry Prism	Block
		1st lift	2nd lift		
Strength, psi (MPa)	2730 (18.82)	4560 (31.44)	5440 (37.51)	3420 (23.85)	3500 (24.13)

All of the steel used for construction was nominally Grade 60. The provided flexural (vertical) reinforcement consisted of No. 6 (M#19) bars and No. 8 (M#25) bars. The provided shear (horizontal) reinforcement consisted of No. 4 (M#13) bars and No. 3 (M#10) bars. Tension tests were performed on coupons of the reinforcement to determine yield strengths and to determine stress-strain curves for use in later computer modeling. The average yield strengths for these steel specimens are given in Table 3.3.

Table 3.3. Tension Yield Strengths

	No. 8 (M#25) Bars	No. 6 (M#19) Bars	No. 4 (M#13) Bars	No. 3 (M#10) Bars
Yield Strength, ksi (MPa)	64 (441)	65 (448)	65 (448)	63 (434)

3.2.4 Wall Specimen Construction

All nine walls were constructed and tested at the Wood Materials and Engineering Laboratory at Washington State University. Footing reinforcing cages, bolt tubes, and the vertical reinforcement starter-bars were all assembled inside wooden forms. Concrete was ordered from a local ready-mix supplier, poured into the forms, and consolidated with a vibrator. To increase friction and reduce wall-sliding, the footprint area of the wall was intentionally roughened with a trowel. To accommodate 7/8 in. (22 mm) diameter steel shear studs used to load the specimens, 2.0 in. (51 mm) diameter holes were cored in masonry units prior to construction. These masonry units were only used in the course at the level of the load application (11th course).

Professional masons constructed all nine wall specimens in running bond with faceshell and web mortar bedding. Shear reinforcement was placed in the bond-beam knockout sections at every other course. On the first day of construction, the first seven courses of each specimen were erected. At the end of this process, the remaining vertical reinforcement was installed. This reinforcement ran the full height of the walls.

On the second day of construction, the first seven courses were grouted and vibrated. Additionally, three more courses were erected (courses 8 through 10), for a total of ten courses.

On the third day of construction, the final three courses were erected (courses 11 through 13). Lateral loading bolts were installed on the 11th course and held in place by two 2x6 boards that prevented grout leakage through the cored holes, as shown in Figure 3.9. Finally, the six remaining ungrouted courses were grouted.

Figure 3.9. Installation of Loading Bolts

3.2.5 Test Setup for Wall Specimens

The specimens were designed with a fixed base to act as a cantilever shear wall. This fixed base condition was achieved by bolting each specimen to a strong floor with eight 1.25 in. (32.0 mm) diameter steel bolts and by securing adjustable steel tube sections between the

columns of the loading frame and each end of the footing in the plane of loading. A 100-kip (445 kN) capacity hydraulic actuator, operated under displacement control, provided the in-plane loading. This actuator was attached to the steel testing frame and applied in-plane load through a load cell and into two steel channels with slotted and oversized holes that were bolted to the shear studs cast-in-place in each wall in the 11th course. The aspect ratio of each wall was 1.76. A picture of the test setup is given in Figure 3.10.

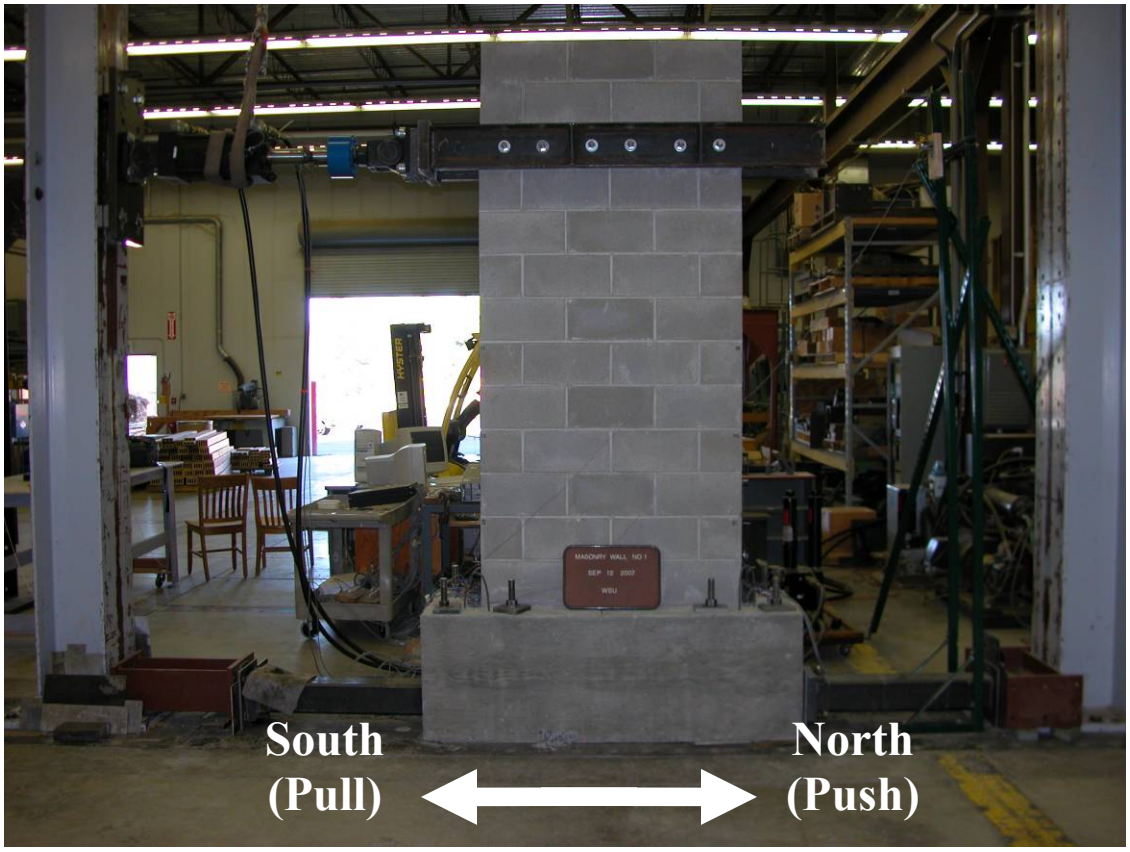

Figure 3.10. Testing Setup - Panels

The directional nomenclature used throughout this paper is as shown in Figure 3.10. Extending the actuator arm caused it to push the wall northward, creating tension in the south toe of the wall. Retracting the actuator arm caused it to pull the wall southward, creating tension in the north toe of the wall.

3.2.6 Instrumentation for Wall Specimens

String potentiometers, strain gages, and a load cell were used to measure and monitor the walls during testing. A string potentiometer attached to the horizontal displacement actuator measured piston displacement and acted as feedback for the actuator control. Another string potentiometer was fixed to a rigid frame disconnected from the testing frame which measured global displacement of the wall in the direction of loading at the height of load application. One strain gage was placed on every vertical reinforcing bar at the footing-to-wall interface and measured strain in the steel along the axis of loading. A load cell was attached to the actuator piston and measured the applied in-plane lateral force.

Additionally, string potentiometers were used to measure the vertical displacements, sliding displacements, and shear displacements of each wall, and strain gages were used to measure the strain in the first two courses of horizontal steel reinforcement of each wall.

3.2.7 System Control and Data Acquisition

Separate computer systems controlled the lateral load application and data acquisition, as shown in Figure 3.11. One computer sent a signal containing a loading rate and a target displacement to the hydraulic controller which provided fluid pressure to the hydraulic actuator. A second computer collected data through a program created in Labview. This program scanned data once every second.

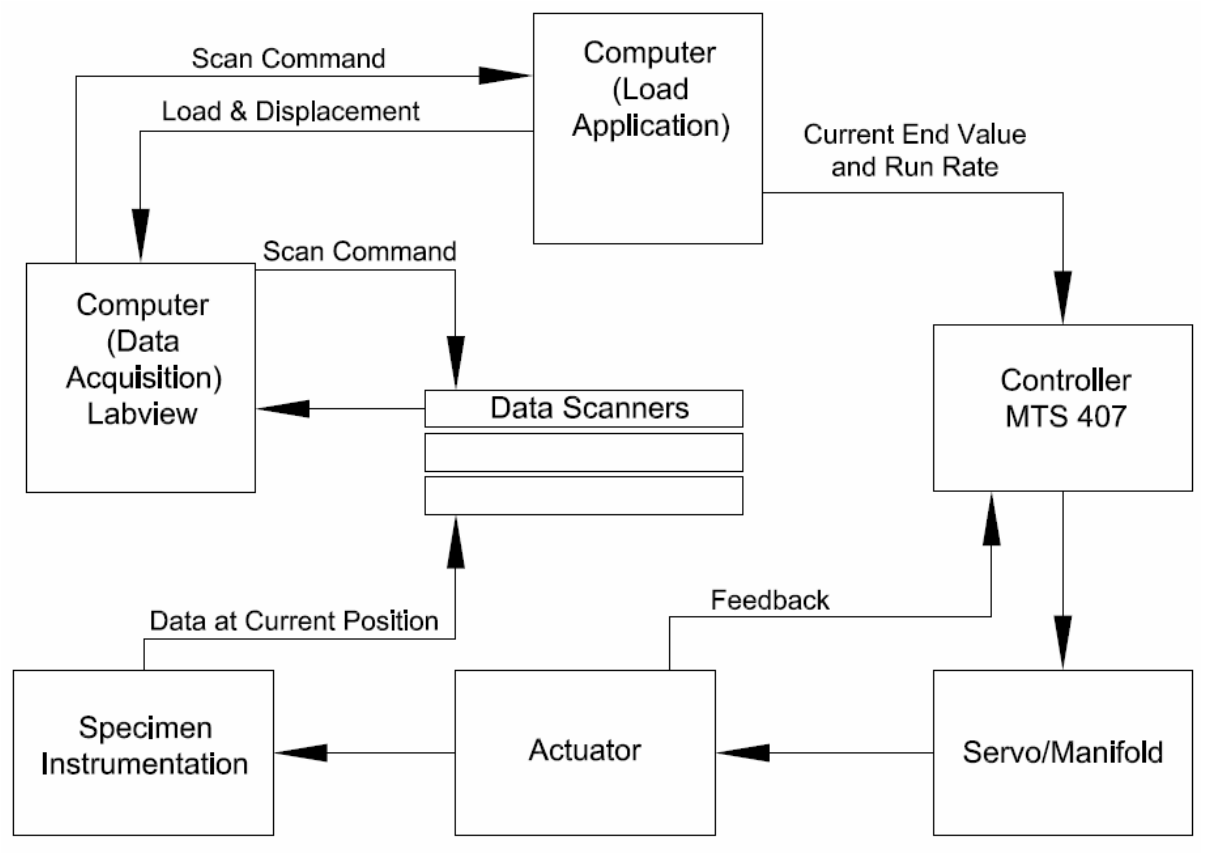

Figure 3.11. Data Acquisition Flow Chart (adapted from Snook, 2005)

3.2.8 Test Procedures for Wall Specimens

All walls were tested under displacement control in the cyclic pattern shown in Figure 3.12. Displacement amplitudes were based on multiples of the theoretical displacement to cause first yielding of the extreme tensile reinforcement bar in each wall. This value is referred to as the first major event (FME) displacement. The FME displacements were calculated for each cross-section using the moment-curvature analysis software, XTRACT. Based on results from this analysis and previous research by Eikanas (2003) and Snook (2005), 0.30 in. (7.62 mm) was used as the FEM displacement for all walls to maintain a uniform testing scheme. Displacement rates were 0.5 in/min (12.7 mm/min) for the first 21

cycles and 1.0 in/min (25.4 mm/min) thereafter until failure. These loading rates produced failure in approximately 1 to 3 hours.

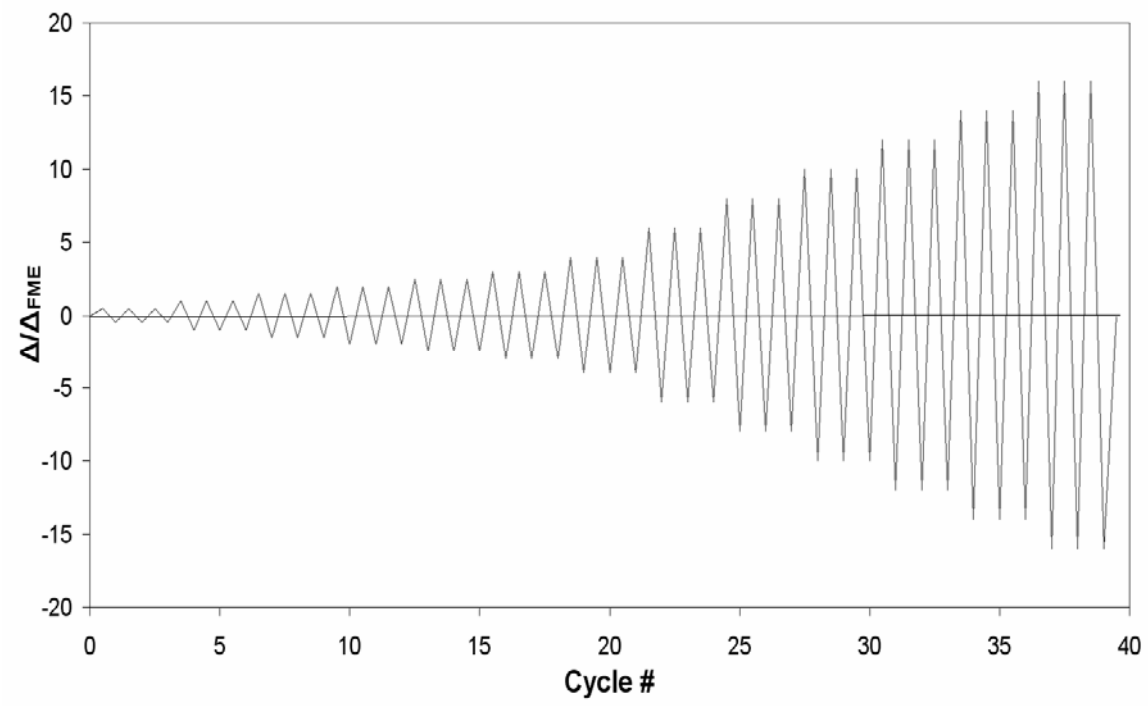

Figure 3.12. Displacement-based Loading Protocol

3.3 Phase II – Panels

Phase II of this research was conducted at Washington State University by a fellow graduate student - Valentine Amar. The primary details and findings of her work are reported here.

3.3.1 Description of Panel Specimens

The panel specimens were constructed of fully grouted masonry in running bond using standard blocks. The provided vertical steel, horizontal steel, and splices of the panel specimens were exactly the same as those provided in the corresponding wall specimens (i.e.

Panel 1 and Wall 1). All walls were three blocks wide and had footprint dimensions of 7.63 in. x 47.6 in. (194 mm x 1209 mm). The height of each wall was such that the full lap length would be enclosed in the grouted cells. Thus, the wall heights varied according to the provided lap within the panel. The panels were constructed such that the vertical reinforcing bars protruded 8 in. (203 mm) from the masonry to allow mechanical coupling to the bars for direct tension testing. A drawing of a typical panel specimen is given in Figure 3.13.

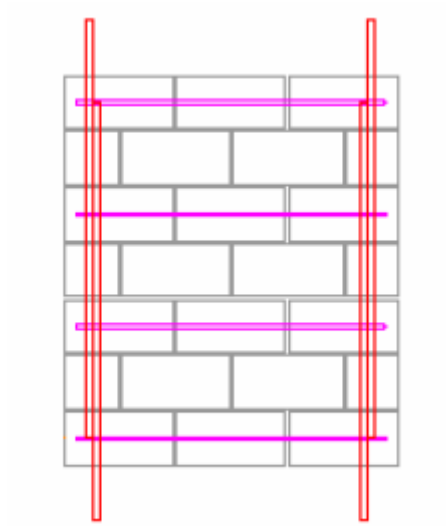

Figure 3.13. Typical Panel Specimen

3.3.2 Material Properties for Panel Specimens

The masonry blocks used for construction were taken from the same stock as those used for the wall specimen construction. Type S mortar was mixed onsite and used for construction. Three test cylinders of the mortar (conforming to ASTM C780), 2 in. (51 mm) diameter by 4 in. (102 mm) height, were made during construction and set aside for testing. 7-sack course aggregate grout was used in the wall specimens. The grouting was completed in two separate lifts; therefore, three grout prisms (conforming to ASTM C1019), 3.5 in. (89 mm) square x 7 in. (178 mm) high, were made from each mix, set aside and capped for

testing. Three block prisms (conforming to ASTM C1314) were made during construction, set aside and capped for testing. These samples were all testing according to ASTM standards, and the average compressive strengths for the materials are given in Table 3.4.

Table 3.4. Compressive Material Strengths - Panels

	Mortar	Grout	Masonry Prism	Block
Strength, psi (MPa)	4185 (28.85)	3640 (25.10)	2620 (18.06)	3500 (24.13)

Note that the compressive strength of the masonry used for the construction of the panels is significantly less than that of the masonry used for the construction of the wall specimens discussed earlier. This reduced masonry strength has an effect on the MSJC required lap length as shown in Table 3.5.

Table 3.5. Provided Laps - Panels

Panels	Bar Size	Length, in. (mm)	d_b	% MSJC Equation	% Simplified Equation	Side Cover, in. (mm)
1	No. 8 (M#25)	48 (1219)	48	69%	100%	3.3 (83.8)
2	No. 8 (M#25)	36 (914)	36	52%	75%	3.3 (83.8)
3	No. 8 (M#25)	36 (914)	36	52%	75%	3.3 (83.8)
4	No. 8 (M#25)	60 (1524)	60	87%	125%	3.3 (83.8)
5	No. 6 (M#19)	36 (914)	48	110%	100%	3.4 (86.4)
6	No. 6 (M#19)	27 (686)	36	82%	75%	3.4 (86.4)
7	No. 6 (M#19)	36 (914)	48	65%	100%	2.0 (50.8)
8	No. 6 (M#19)	27 (686)	36	48%	75%	2.0 (50.8)
9	No. 6 (M#19)	45 (1143)	60	81%	125%	2.0 (50.8)

All of the steel bars used for construction were taken from the same stock as those used for the wall specimen construction. The average yield strengths for these steel specimens are given earlier in Table 3.3.

3.3.3 Panel Specimen Construction

All nine panels were constructed and tested in the Wood Materials and Engineering Laboratory at Washington State University. Professional masons constructed all nine panel specimens in running bond with faceshell and web mortar bedding. Panels were constructed upright on wooden platforms to allow for the vertical reinforcement to protrude 8 in. (203 mm) from the base of the wall.

Shear reinforcement was placed in the bond-beam knockout sections at every other course. On the first day of construction, the mortar and block of all nine specimens was erected and the lapped bars were dropped into the cells and positioned. On the second day of construction, all nine specimens were fully grouted and vibrated.

3.3.4 Test Setup for Panel Specimens

The testing setup consisted of a steel frame, mechanical couplers, two hydraulic jacks, and a hydraulic control. A drawing of the test setup is given in Figure 3.14. A mechanical coupler was fitted onto each piece of protruding reinforcement and tightened thoroughly. High-strength rods (threaded on each end) were threaded into the opposite ends of each coupler. These high-strength rods were anchored to one side of the testing frame with a nut and washers. On the other side of the panel, they were connected in a similar manner to hydraulic jacks that supplied load to the specimen. The jacks were connected in parallel to ensure that each splice was subject to an approximately equal load.

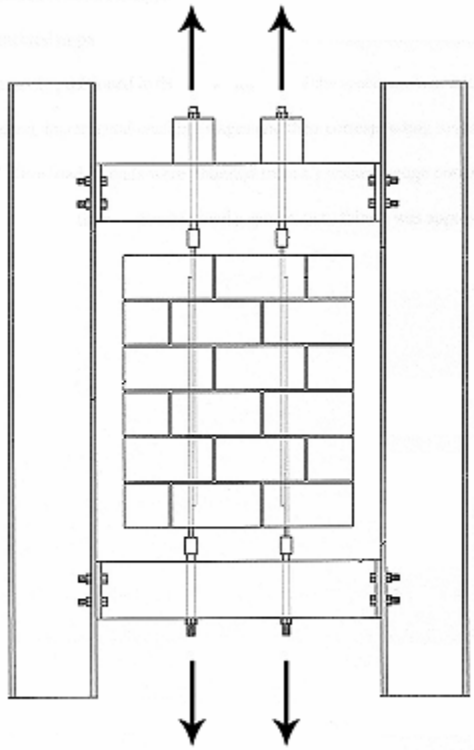

Figure 3.14. Testing Setup - Panels

3.3.5 System Control, Data Acquisition, and Test Procedures

Once the specimen was securely positioned in the frame, the hydraulic control was activated and loading of the specimen began. Changes in fluid pressure were controlled manually with a dial, and loads were obtained visually from a pressure gage with 10 ksi (69 MPa) capacity connected to the hydraulic pump. The average total time required to load a specimen to failure was approximately 5 minutes. Load at final failure was recorded for each specimen.

CHAPTER 4: RESULTS OF TESTING

4.1 Introduction

In this chapter, results are presented for each of the nine shear wall tests and nine direct tension panel tests. Information presented includes test observations, wall load-displacement measurements, and peak tensile stresses of the spliced flexural reinforcement.

4.2 Phase I – Results of Wall Testing

For brevity, failure pictures, load-displacement hysteresis curves, and full discussion are provided for only three representative walls in this section. A complete set of the nine load-displacement hysteresis curves is presented in the Appendix. For seven of the nine walls tested, the ultimate failure mechanism was identical for both the north and south sides of the walls. For the two walls that exhibited different ultimate failure mechanisms (Wall 4 and Wall 5), there is strong correlation between the peak applied lateral loads for the north and south sides. For these reasons, the data from the north and south sides of each wall are presented as average values in this report following the discussion of the three representative walls.

4.2.1 Typical Ultimate Failure Mechanism

All walls exhibited similar ultimate failure characteristics. Of the eighteen wall sides tested (two per wall), sixteen exhibited lap failures concurrent with a significant decrease in load and some degree of longitudinal splitting of the masonry assemblage. Typically, hairline radial cracks developed slowly over a number of cycles on the masonry faceshell nearest the internal lapped bars. Depending on the lap detailing, these hairline radial cracks would grow

to between 3 and 8 in. (76 and 203 mm) before the point of peak load resistance and corresponding lap failure. When a lap splice failed, the longitudinal splitting was often sudden and dramatic, creating an “unzipping” effect as the crack developed from the tip of an existing radial crack to the top of the lap. A significant drop in load was observed every time a lap failed from this “unzipping” effect of longitudinal splitting of the masonry assemblage.

4.2.2 Wall 1 - No. 8 (M#25) bars, 48 d_b

Wall 1 was constructed using a single No. 8 (M#25) bar in each of the outer cells. The provided lap splices were 48 bar diameters (48 in., 1219 mm), or 100% and 79% of the required lap according to Equation 2.1 and Equation 2.2, respectively.

Test Observations: A picture of Wall 1 displaying cracking and lap failures is shown in Figure 4.1. Between the 10th and 18th cycles, hairline cracks developed on the masonry faceshell of all four wall corners nearest the internal lapped bars. A typical hairline radial crack is shown in Figure 4.2. On the 19th cycle (+/- 1.8 in. displacement (+/- 45.7 mm)), for each direction of loading, the tension laps failed in a dramatic fashion according to the longitudinal splitting effect previously described. These lap failures corresponded with the hairline radial cracks nearest the tension lap “unzipping” to the top of the lap and a significant drop in load.

Figure 4.1. Cracking and Lap Failures - Wall 1

Figure 4.2. Hairline Radial Crack - Wall 1

Load-Displacement: The load-displacement hysteresis curves for Wall 1 are shown in Figure 4.3. Abrupt lap failures in the load-displacement hysteresis curves are characterized by the straight line segments illustrating sharp decline in load with minimal change in displacement.

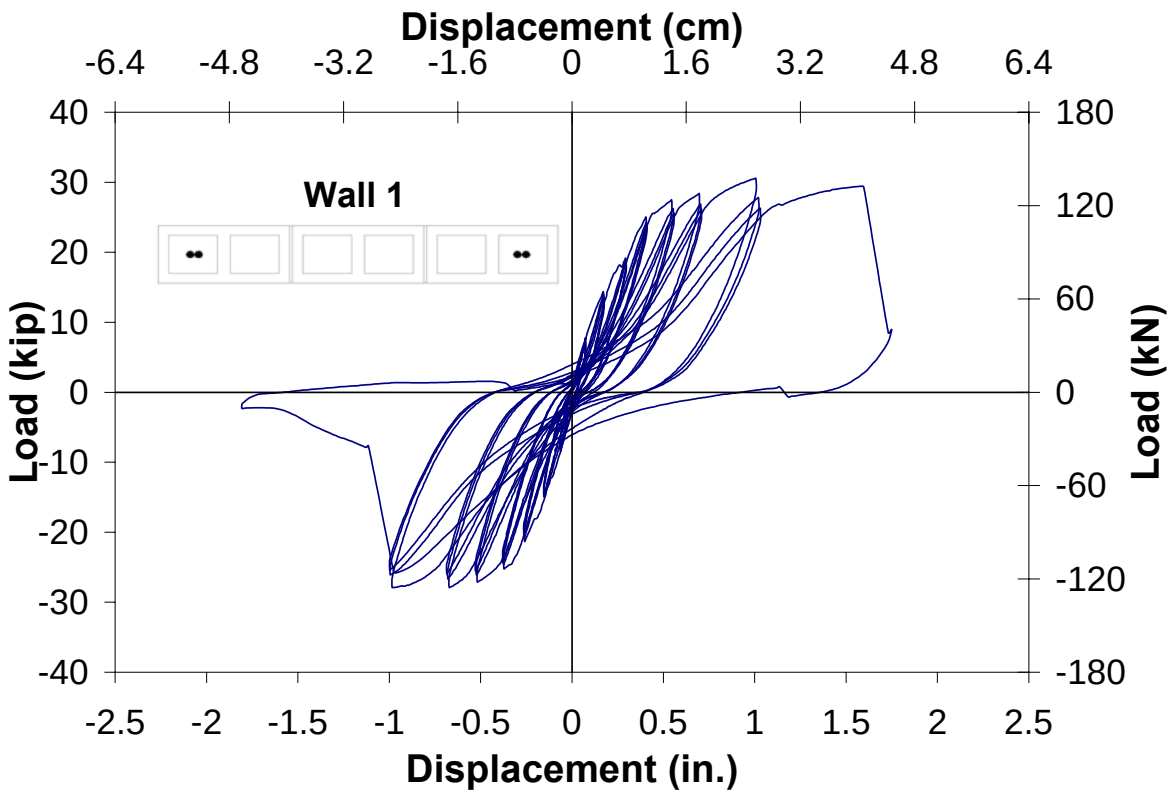

Figure 4.3. Load-Displacement Hysteresis Curves; Wall 1

4.2.3 Wall 5 - No. 6 (M#19) bars distributed, 48 d_b

Wall 5 was constructed using No. 6 (M#19) bars in the first and second cells of each side. The provided laps were 48 bar diameters (36 in. (914 mm)), or 100% and 125% of the required lap according to Equation 2.1 and Equation 2.2, respectively.

Test Observations: A picture of Wall 5 displaying cracking and lap failure is shown in Figure 4.4. Wall 5 is one of only two walls that exhibited toe crushing and gradual load

degradation. During the 18th cycle, visual observation of cracks on the south toe of the wall suggested the onset of toe crushing. Almost no radial cracks were visible until the 20th cycle when a significant radial crack developed through 4.5 courses on the south side of the wall. Thus, by examining the south toe of Wall 5, it is possible to identify both the toe crushing and the gradual load degradation causing failure in the pull direction as well as the abrupt lap failure causing failure in the push direction.

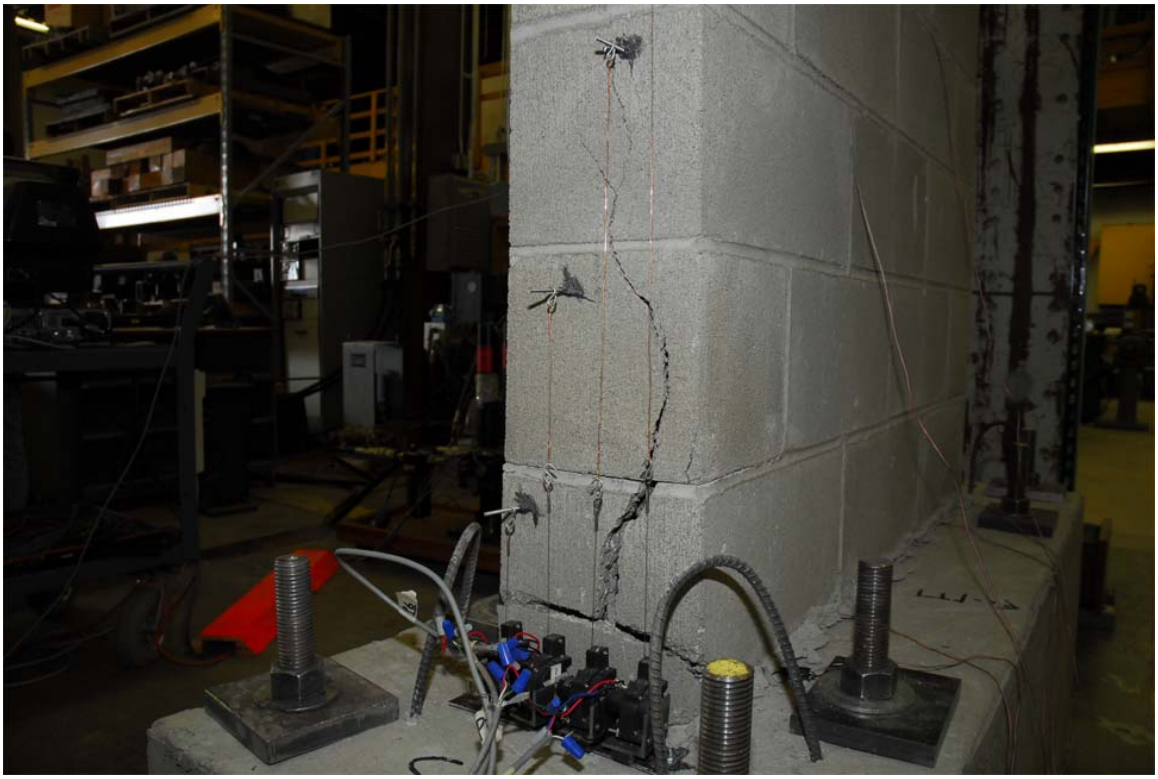

Figure 4.4. Cracking and Lap Failure - Wall 5

Load-Displacement: The load-displacement hysteresis curves for Wall 5 are shown in Figure 4.5.

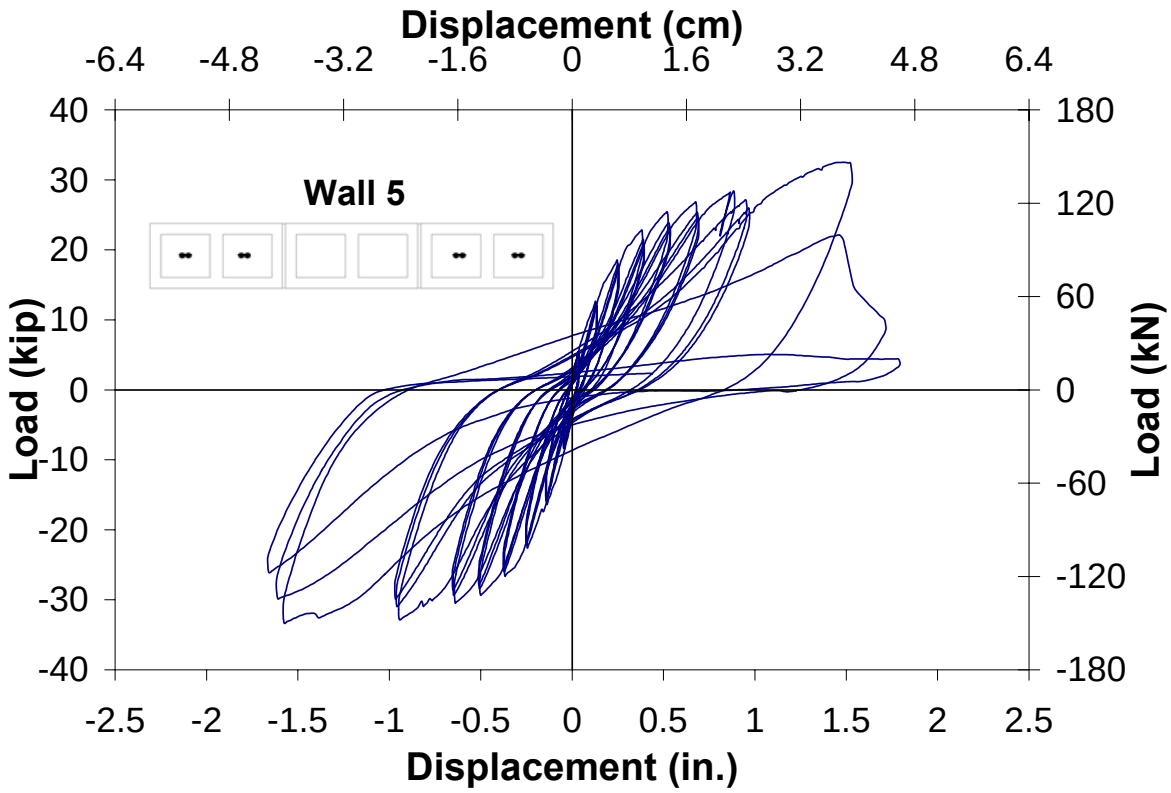

Figure 4.5. Load-Displacement Hysteresis Curves - Wall 5

4.2.4 Wall 7 - No. 6 (M#19) bars offset, 48 d_b

Wall 7 was constructed using two No. 6 (M#19) bars in each of the outer cells. The provided laps were 48 bar diameters (36 in. (914 mm)), or 100% and 74% of the required lap according to Equation 2.1 and Equation 2.2, respectively.

Test Observations: A picture of Wall 7 displaying cracking and lap failure is shown in Figure 4.6. Between the 10th and 15th cycles, hairline cracks developed on the masonry faceshell of all four wall corners nearest the internal lapped bars. While pulling towards the south during the 16th cycle (- 0.9 in. displacement (- 22.9 mm)), the tension laps in the north side of the wall failed in a sudden fashion as a result of the longitudinal splitting effect previously described. These lap failures corresponded with the hairline radial cracks nearest

the tension lap "unzipping" to the top of the lap and a significant drop in load. A similar event was noticed on the south side of the wall while pushing towards the north during the 19th cycle (+ 1.2 in. displacement (+ 30.5 mm)).

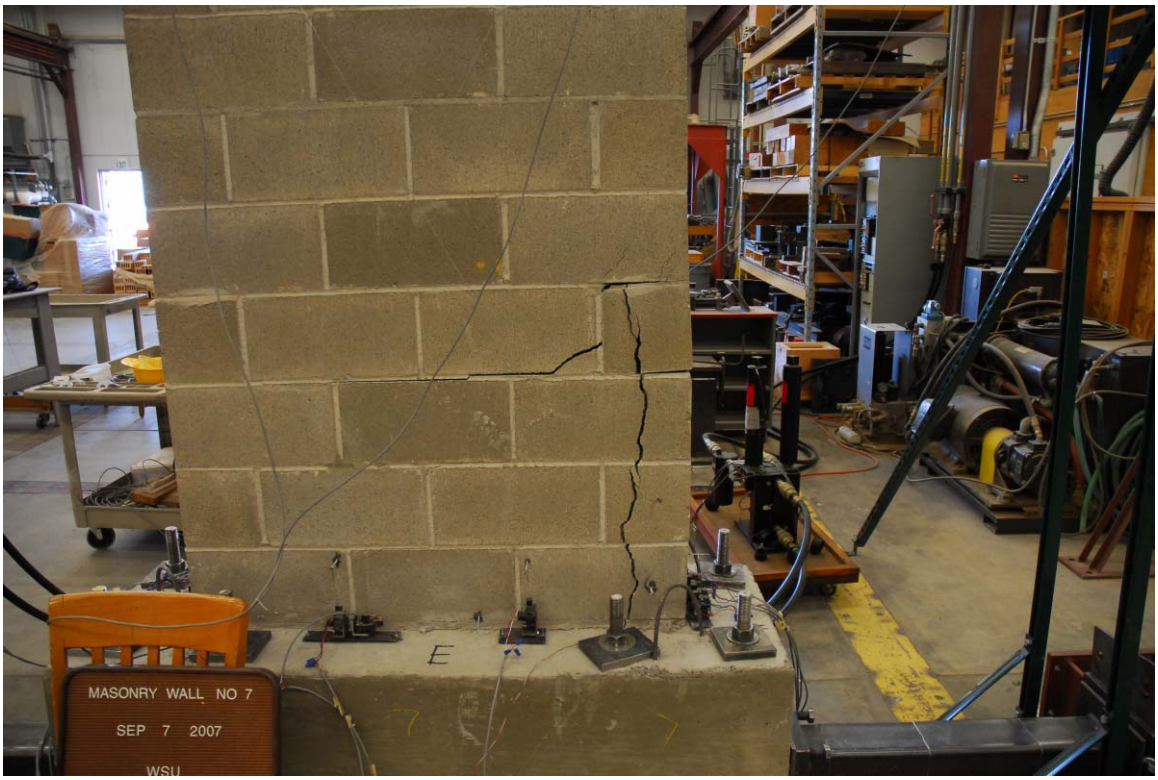

Figure 4.6. Cracking and Lap Failure - Wall 7

Load-Displacement: The load-displacement hysteresis curves for Wall 7 are shown in Figure 4.7. Note that an abrupt drop in load occurs very early in testing.

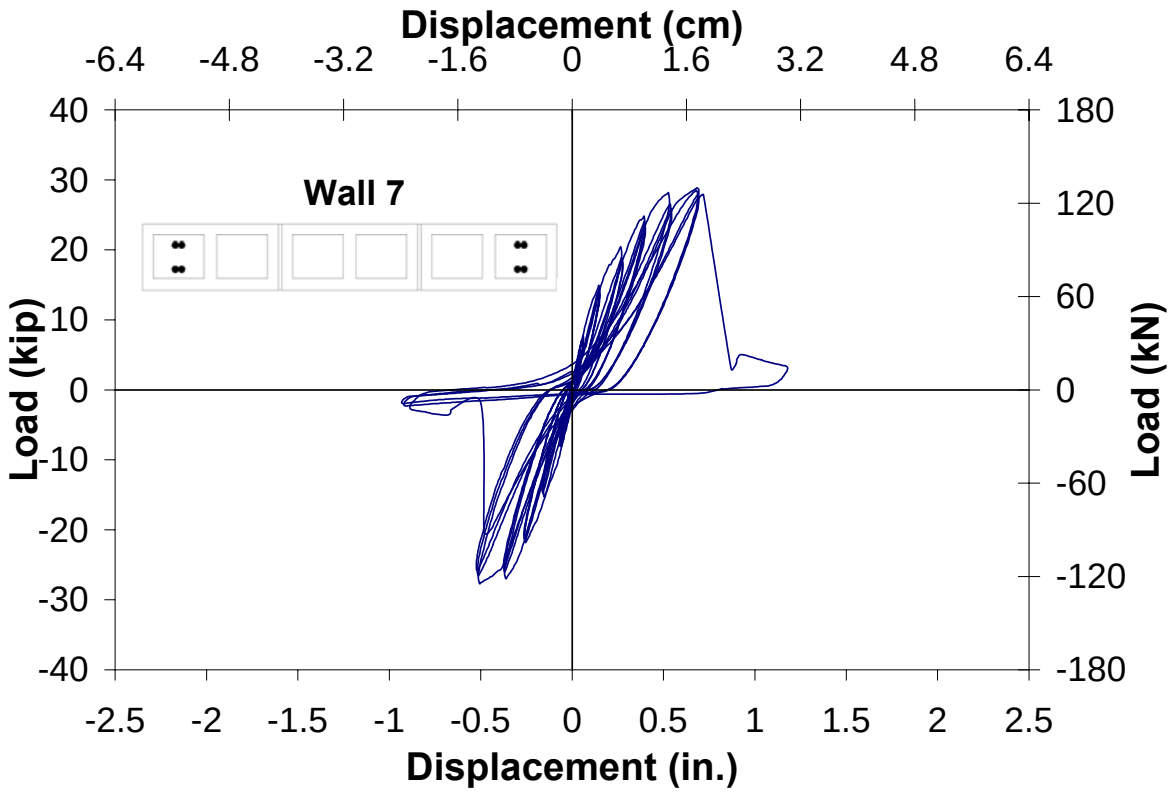

Figure 4.7. Load-Displacement Hysteresis Curves - Wall 7

4.2.5 Reinforcement Stresses at Failure in Wall Specimens

Of the twenty-eight strain gages installed on the lapped longitudinal reinforcing bars, only seven survived and were functioning at the point of peak load. Moment-curvature analysis was performed on all three wall cross-sections using actual material properties. The product of an applied load during physical testing and the height of the load application can be related to a specific moment from the moment-curvature analysis. Using this relationship as the bridge between results from physical testing and computer modeling, the seven valid strain data from testing were used to compare measured strains with values from the moment-curvature analysis (theoretical). The average difference between the theoretical and

measured strain values was 2%, indicating good agreement between the moment-curvature analysis and the test data.

Table 4.1 provides a summary of the peak stresses in the lapped bars for the nine walls of this study, expressed as a ratio of the developed stress to the specified yield strength of the reinforcement. Results clearly indicate that as the provided lap length increased, the developed stresses in the flexural reinforcement increased.

Walls 1 and 5 each contained lap lengths of 48 bar diameters and achieved a stress ratio of at least 1.25. Therefore, for walls with No. 8 (M#25) or No. 6 (M#19) bars centered in the cells and containing transverse reinforcement consisting of No. 4 (M#13) bars spaced at 16 in. (406 mm) on center, the simplified equation of 48 bar diameters (Equation 2.1) is sufficient for lap splice design.

Comparisons of the developed stresses of Walls 5 through 9 indicate that lap splices in walls with reduced cover (resulting from offsetting bars in the cells) are likely to fail at lower stresses than similar laps centered in the cells. For example, the 45 in. (1143 mm) lap in Wall 9 developed less stress than the 27 in. (686 mm) lap in Wall 6.

Table 4.1. Ratios of Developed Stress and Specified Yield Stress - Walls

Walls	Bar Size	Length, in. (mm)	d_b	% MSJC Equation	% Simplified Equation	Stress, ksi (Mpa)	$\sigma_{developed}/F_y$
1	No. 8 (M#25)	48 (1219)	48	79%	100%	74.85 (516.1)	1.25
2	No. 8 (M#25)	36 (914)	36	59%	75%	68.25 (470.6)	1.14
3	No. 8 (M#25)	36 (914)	36	59%	75%	69.20 (477.1)	1.15
4	No. 8 (M#25)	60 (1524)	60	99%	125%	79.75 (549.9)	1.33
5	No. 6 (M#19)	36 (914)	48	125%	100%	76.95 (530.6)	1.28
6	No. 6 (M#19)	27 (686)	36	94%	75%	71.55 (493.3)	1.19
7	No. 6 (M#19)	36 (914)	48	74%	100%	65.75 (453.3)	1.10
8	No. 6 (M#19)	27 (686)	36	55%	75%	57.95 (400.0)	0.97
9	No. 6 (M#19)	45 (1143)	60	92%	125%	69.35 (478.2)	1.16

4.2.6 Backbone Curves

Backbones of load-displacement hysteresis curves offer clear comparisons between walls with respect to peak load resistance and displacement ductility. A single backbone curve is presented for each wall and represents the average of the backbone curves from each wall side. The three graphs presented in this section are plotted on the same scale.

Graphs of the backbones of the load-displacement hysteresis curves for Walls 1 through 4 are given in Figure 4.8. Increased lap lengths resulted in improvements with respect to displacement capacity and ultimate load resistance.

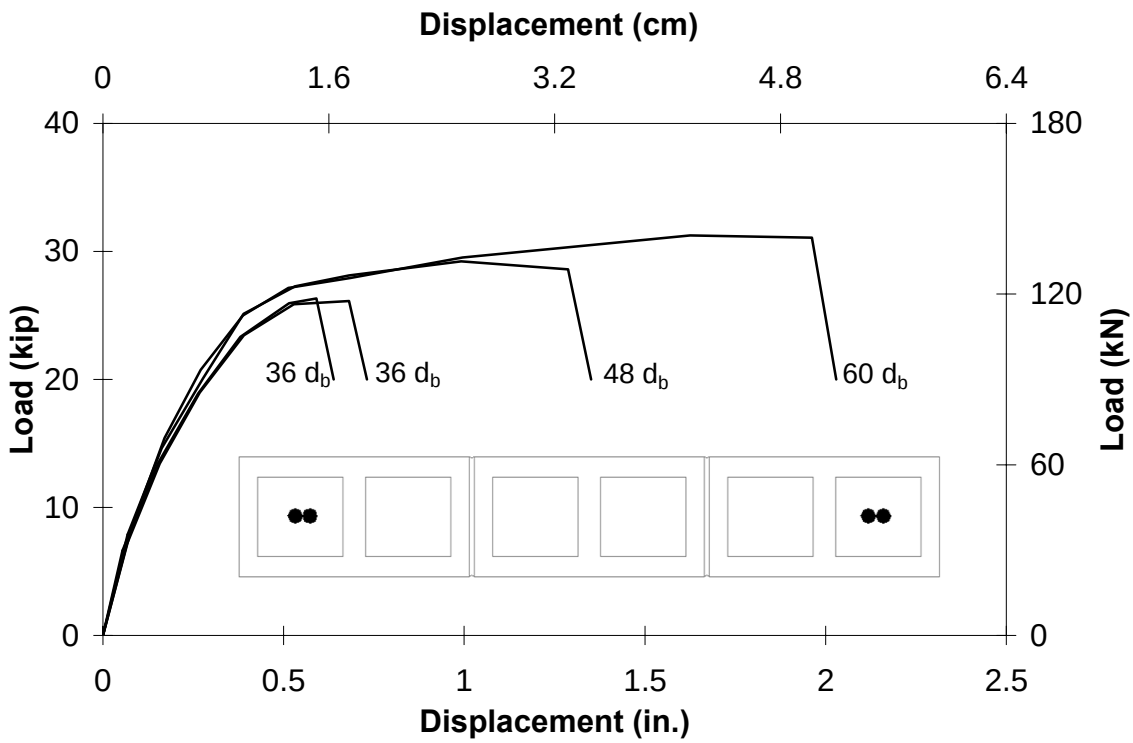

Figure 4.8. Backbone Curves - Walls 1-4

Graphs of the backbone of the load-displacement hysteresis curves for Walls 5 and 6 are given in Figure 4.9. Increased lap lengths resulted in improvements with respect to displacement capacity and ultimate load resistance.

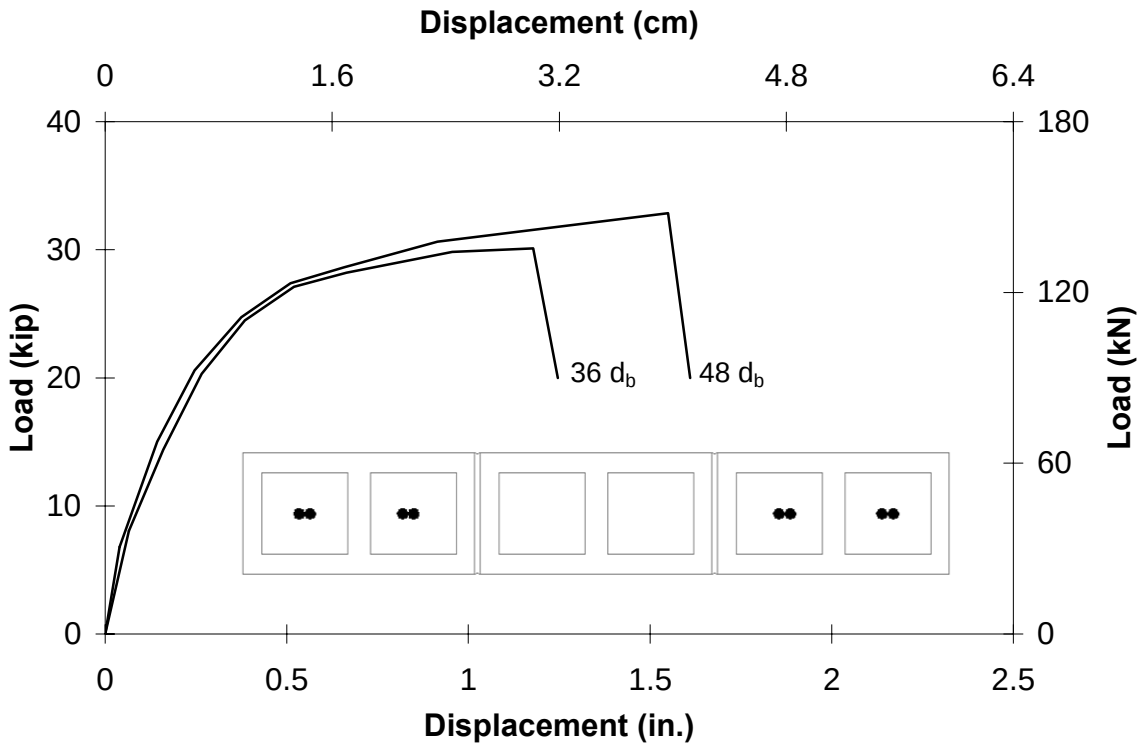

Figure 4.9. Backbone Curves - Walls 5-6

Graphs of the backbone of the load-displacement hysteresis curves for Walls 7 through 9 are given in Figure 4.10. It is clear that these walls performed quite poorly with respect to ultimate load resistance and displacement capacity compared to walls of the previous set containing similar lap lengths. The performance of Wall 9 (60 d_b laps) is comparable to the performance of Wall 6 which utilized much smaller 36 d_b laps. The lesser performance of the splices in Walls 7, 8 and 9 is a direct result of reduced clear cover.

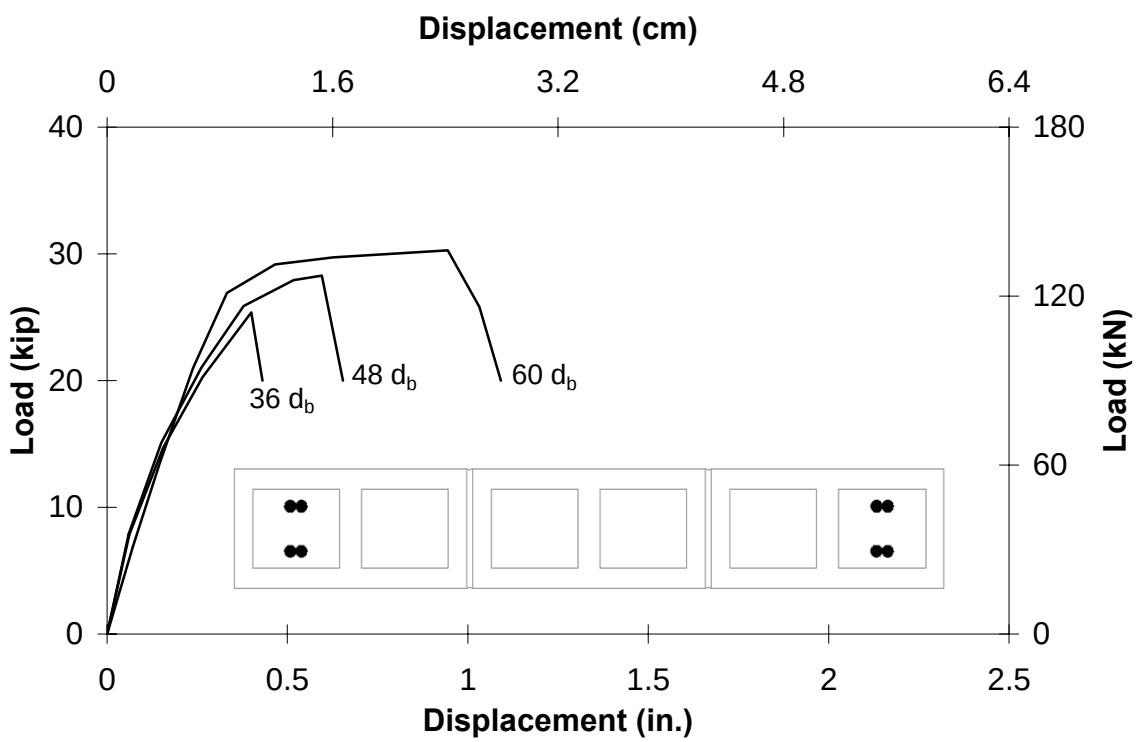

Figure 4.10. Backbone Curves - 7-9

4.3 Phase II – Results of Panel Testing

4.3.1 Typical Ultimate Failure Mechanism

All nine panels exhibited lap failures concurrent with an immediate decrease in load and some degree of longitudinal splitting of the masonry assemblage. Because of the

uniformity of failure characteristics of the panels tested and the detail of discussion given to this subject in a number of previous reports, a failure picture and discussion will only be provided for a single panel.

4.3.2 Testing Irregularities

Although every attempt was made to construct symmetric and consistent test specimens, small but common variations in the panels resulted in slightly nonuniform specimens. As a result, one splice failed before the other in all walls.

During the testing of Panel 4, the mechanical couplers on the No. 8 (M#25) bars failed prematurely. The strength of the connection was limited by the strength of the hand-tightened bolts used to anchor the coupler to the bar. As such, the splices in Panel 4 did not fail and the results presented reflect the peak stress reached before the couplers failed.

4.3.3 Panel 9 - No. 6 (M#19) bars offset, 60 d_b

Panel 9 was constructed using two No. 6 (M#19) bars in each of the outer cells. The provided laps were 60 bar diameters (45 in., 1143 mm), or 125% and 92% of the required lap according to Equation 2.1 and Equation 2.2, respectively.

Test Observations: A picture of Wall 9 displaying cracking and lap failure is shown in Figure 4.11. Cracking prior to failure in the panel was significantly less than the cracking observed during the cyclic test of Wall 9. However, the cracking after failure was much more dramatic as the entire portion of the wall outside the lapped bars broke off.

Figure 4.11. Cracking and Lap Failure; Panel 9

4.3.4 Reinforcement Stresses at Failure in Panel Specimens

Table 4.3 provides a summary of the peak stresses in the lapped bars for the nine panels of this study, expressed as a ratio of the stress to the specified yield strength of the reinforcement. Because the panel specimens had a different strength of masonry assemblage than the wall specimens, the required MSJC lap lengths are different than those given in Table 4.1. Results indicate that as the provided lap length increased, the developed stresses in the flexural reinforcement increased.

Comparisons of the developed stresses of Panels 5 through 9 indicate that lap splices in walls with reduced cover (resulting from offsetting bars in the cells) are likely to fail at lower stresses than similar laps centered in the cells. For example, the 45 in. (1143 mm) lap in Panel 9 developed nearly the same stress as the 27 in. (686 mm) lap in Panel 6.

Table 4.3. Ratios of Developed Stress and Specified Yield Stress - Panels

Panels	Bar Size	Length, in. (mm)	d_b	% MSJC Equation	% Simplified Equation	Stress, ksi (Mpa)	$\sigma_{developed}/F_y$
1	No. 8 (M#25)	48 (1219)	48	69%	100%	72.15 (497.5)	1.20
2	No. 8 (M#25)	36 (914)	36	52%	75%	61.52 (424.2)	1.03
3	No. 8 (M#25)	36 (914)	36	52%	75%	62.66 (432.0)	1.04
4	No. 8 (M#25)	60 (1524)	60	87%	125%	77.47 (534.1)	1.29
5	No. 6 (M#19)	36 (914)	48	110%	100%	76.36 (526.5)	1.27
6	No. 6 (M#19)	27 (686)	36	82%	75%	73.64 (507.7)	1.23
7	No. 6 (M#19)	36 (914)	48	65%	100%	62.05 (427.8)	1.03
8	No. 6 (M#19)	27 (686)	36	48%	75%	51.14 (352.6)	0.85
9	No. 6 (M#19)	45 (1143)	60	81%	125%	74.32 (512.4)	1.24

4.4 Conclusions

For the walls tested in this study, increased lap lengths resulted in significant improvements with respect to displacement capacity and ultimate load resistance. For the

panels and walls tested, increased lap lengths resulted in increased developed stresses in the longitudinal reinforcement.

For walls with No. 8 (M#25) or No. 6 (M#19) bars centered in the cells and containing transverse reinforcement consisting of No. 4 (M#13) bars spaced at 16 in. (406 mm) on center, the simplified equation (Equation 2.1) was sufficient to achieve satisfactory lap splice performance.

The effects of reduced masonry cover must be considered for lap splice design. Results indicate that lap splices in specimens with reduced cover (resulting from offsetting bars in the cells) are likely to fail at lower stresses than similar laps centered in the cells. The poor performance of specimens 7, 8 and 9 is a direct result of reduced clear cover.

CHAPTER 5: ANALYSIS AND DISCUSSION OF TEST RESULTS

5.1 Introduction

This chapter provides evaluations of the performance of reinforcement lap splices in concrete masonry shear walls subjected to in-plane lateral loading and in concrete masonry panels subjected to direct tension. Evaluations were based on comparisons between the two testing phases as well as comparisons to lap splice design equations. For each of the figures in this section, specimens were grouped according to the reinforcement pattern, with best-fit lines provided for each group of data.

5.2 Comparison of Testing Methods

A numerical comparison of the developed stresses for the walls and panels tested is presented in Table 5.1. Percent errors were calculated using the data from the wall testing as the accepted values. The data presented in this table provides a means of comparing the two testing methods directly. However, a direct comparison of these developed stresses does not take into account the difference in masonry compressive strength between the two specimen types. Although construction of the two specimen types was intended to yield two sets of masonry with identical compressive strengths, recall that the masonry compressive strength of the walls was larger than that of the panels by 800 psi (5.52 MPa). Despite this difference, a direct comparison is still the best means of comparing the two methods of testing.

Table 5.1. Comparison of Developed Stresses

Wall or Panel	Bar Size	Length, in. (mm)	d_b	% MSJC Equation	% Simplified Equation	$\sigma_{developed}/F_y$		% Error
						Walls	Panels	
1	No. 8 (M#25)	48 (1219)	48	79%	100%	1.25	1.20	-3.6%
2	No. 8 (M#25)	36 (914)	36	59%	75%	1.14	1.03	-9.9%
3	No. 8 (M#25)	36 (914)	36	59%	75%	1.15	1.04	-9.5%
4	No. 8 (M#25)	60 (1524)	60	99%	125%	1.33	1.29	-2.9%
5	No. 6 (M#19)	36 (914)	48	125%	100%	1.28	1.27	-0.8%
6	No. 6 (M#19)	27 (686)	36	94%	75%	1.19	1.23	2.9%
7	No. 6 (M#19)	36 (914)	48	74%	100%	1.10	1.03	-5.6%
8	No. 6 (M#19)	27 (686)	36	55%	75%	0.97	0.85	-11.8%
9	No. 6 (M#19)	45 (1143)	60	92%	125%	1.16	1.24	7.2%

The greatest difference between the two testing methods for a given configuration is 11.8% for Wall 8 and Panel 8. The smallest difference between the two testing methods for a given configuration is 0.8% for Wall 5 and Panel 5. In the context of performing structural tests of this nature, some scatter of the data is inherent. The average percent error for the nine configurations is 3.8%, with the walls producing slightly larger values on average. This value suggests there is little difference between the two testing methods with respect to splice capacity.

5.3 Comparisons with Simplified Equation

A plot of the provided lap length, expressed as a percentage of the simplified equation (Equation 2.1), versus the ratio of developed stress to specified yield stress is given in Figure 5.1 for the walls and panels tested. Three trend lines are presented in the graph, one for each group of specimens based on the provided configuration of longitudinal reinforcement. The trend line for the specimens containing No. 6 (M#19) bars offset in the cells crosses the vertical 48-d_b-axis at a stress ratio of 1.05. The difference between 1.05 and 1.25 is approximately 16%; thus, for walls with reduced cover (from offsetting bars in the cells), the simplified equation significantly overestimates the splice capacity. This confirms the need to address cover for lap splice design.

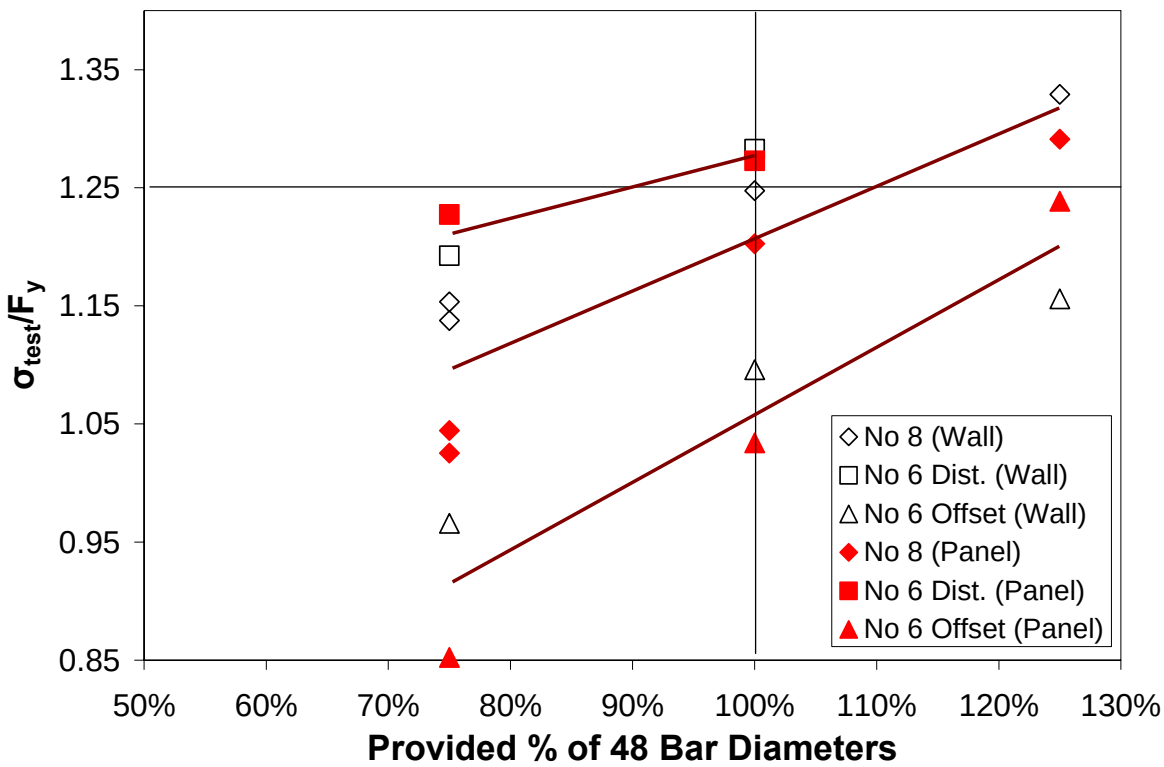

Figure 5.1. Provided % of 48 d_b versus σ_{Test}/F_y - Walls & Panels

5.4 Comparisons with Current MSJC Equation

A plot of the provided lap length, expressed as a percentage of the MSJC equation (Equation 2.2), versus the ratio of developed stress to specified yield stress is given in Figure 5.2 for the walls and panels tested. Three trend lines are presented in the graph, one for each group of specimens based on the provided configuration of longitudinal reinforcement. Values where the linear extensions of the best-fit lines cross the two axes are given in Table 5.2.

The trend line for the specimens containing No. 6 (M#19) bars offset in the cells crosses the horizontal 1.25-axis at 94% of the MSJC equation. This result indicates that the MSJC code may be conservative by 6% for such a configuration. However, these specimens achieved a stress ratio of 1.29 when provided with lap lengths corresponding to 100% of the MSJC equation. This value is within 4% of the target value of 1.25, indicating that the MSJC equation is effective at predicting the behavior of lap splices with reduced masonry cover.

The trend line for the specimens containing No. 8 (M#25) bars crosses the horizontal 1.25-axis at 81% of the MSJC equation. This result indicates that the MSJC equation may be conservative by nearly 20% for the specimens tested containing No. 8 (M#25) bars. The better-than-predicted performance may be due to beneficial effects of the provided horizontal reinforcement, although it should be noted that no such gains were recorded for the specimens containing No. 6 (M#19) bars centered in the cells.

The trend line for the specimens containing No. 6 (M#19) bars centered in the cells crosses the horizontal 1.25-axis at 107% of the MSJC equation, suggesting it is unconservative by 7% for such configurations. However, these specimens achieved a stress

ratio of 1.24 when provided with lap lengths corresponding to 100% of the MSJC equation. This value is within less than 1% of the target value of 1.25, indicating that the MSJC equation is effective at predicting the behavior of lap splices with No. 6 (M#19) bars centered in the cells.

In summary, the current MSJC requirements predicted the performance of lap splices for No. 6 (M#19) bars centered and offset in the cells with reasonable accuracy. However, the provisions appear to be overly conservative for lap splices of No. 8 (M#25) bars by roughly 20%; this may be a result of confinement provided by transverse reinforcement in the walls. These results also suggest that perhaps little or no benefit was provided by the transverse reinforcement for walls containing No. 6 (M#19) bars.

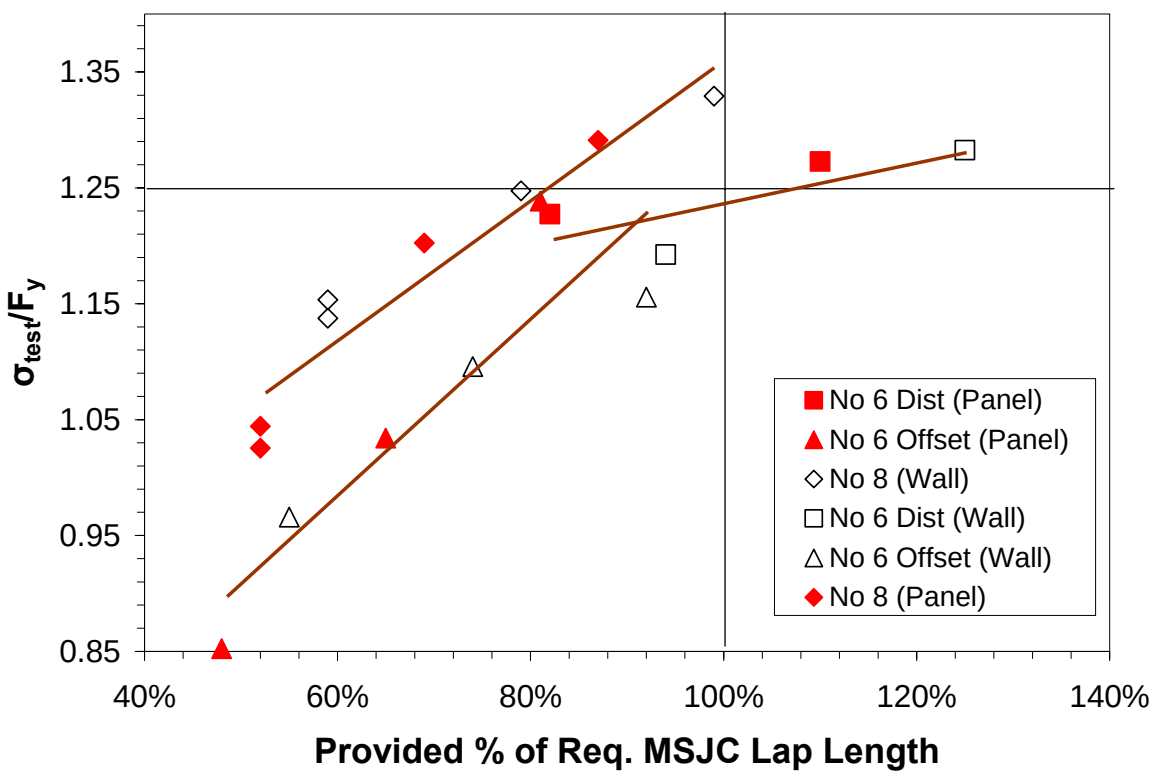

Figure 5.2. Provided % of Req. MSJC Lap Length versus σ_{Test}/F_y - Walls & Panels

Table 5.2. Values where Extensions of Best-Fit Lines Cross Axes – Walls & Panels

Group of Specimens w/ Similar Reinforcement Pattern	Value where extension of best-fit line crosses the:	
	vertical 100%-axis	horizontal 1.25-axis
No. 8 Bars	1.36	81%
No. 6 Bars Distributed	1.29	94%
No. 6 Bars Offset	1.24	107%

5.5 Confinement Effects of Different Transverse Reinforcement Details

It was hypothesized that different detailing of the transverse reinforcement may improve the confining effects from the transverse reinforcement prompting the inclusion of Wall 3 in this study. Wall 3 is identical to Wall 4, the only exception being the provided transverse reinforcement; two No. 3 (M#10) bars were provided instead of a single No. 4 (M#13) bar. The results from this study indicated no difference in results by providing one over the other. The peak stresses achieved in the lapped reinforcement for Walls 3 and 4 and for Panels 3 and 4 are within less than 1% of each other. Broadly applied, these results indicate that a single transverse reinforcing bar provides the same effect to a lap splice as an equivalent area of transverse steel distributed among two bars.

CHAPTER 6: CONCLUSIONS

6.1 Summary

This research investigated the performance of reinforcement lap splices in concrete masonry incorporating common reinforcing details and loaded until failure in in-plane flexure and direct tension for wall specimens and panel specimens, respectively. Variables investigated in this study include length of lap, size of bar, concentrated versus distributed reinforcement, reduced cover resulting from bars offset in the cells, and method of testing. Nine concrete masonry shear walls incorporating flexural reinforcement lap splices at the bases of the walls were constructed and subjected to in-plane cyclic loading. Additionally, nine concrete masonry panels incorporating identical lap splices were constructed and subjected to direct tension. Evaluations of the performance of lap splices were based on comparisons between the two testing phases as well as comparisons to code requirements.

6.2 Conclusions

Effects of Testing Method on Lap Performance - There appear to be no significant differences in the performance of a lap splice tested in direct tension and in-plane flexure. This finding supports the validity of the large amount of data and resulting code equation based on direct tension loading of lap splices.

Effects of Reduced Masonry Cover on Lap Performance - Reduced masonry clear cover significantly affects lap performance. The walls containing No. 6 (M#19) bars offset in the cells performed poorly with respect to ultimate load resistance and displacement capacity compared to walls with similar amounts of reinforcing distributed in the center of the cells,

even when provided with relatively long lap lengths. Additionally, the lapped bars in the walls and panels with reduced masonry cover achieved significantly lower peak stresses than lapped bars in the walls and panels with similar amounts of reinforcing distributed in the center of the cells. This confirms the need to address cover for lap splice design, supporting the MSJC equation and undermining the simplified equation.

Simplified Equation - For walls with No. 8 (M#25) or No. 6 (M#19) bars centered in the cells and containing transverse reinforcement consisting of No. 4 (M#13) bars spaced at 16 in. (406 mm) on center, the simplified equation of 48 bar diameters (Equation 2.1) is sufficient for lap splice design. For walls and panels with reduced cover (from offsetting bars in the cells) the simplified equation significantly overestimates splice capacity.

2005 MSJC Equation - For the parameters considered in this study, the current MSJC requirements predicted the performance of lap splices for No. 6 (M#19) bars centered and offset in the cells with reasonable accuracy. However, the provisions appear to be overly conservative for lap splices of No. 8 (M#25) bars by roughly 20%; this may be a result of confinement provided by transverse reinforcement in the walls. These results also suggest that perhaps little or no benefit was provided by the transverse reinforcement for walls containing No. 6 (M#19) bars.

Confinement Effects of Transverse Reinforcement Distribution - A single transverse reinforcing bar provides the same confinement benefits to a lap splice as an equivalent area of transverse steel distributed among two bars.

REFERENCES

American Society for Testing and Materials: 2005. *Annual Book of ASTM Standards*, West Conshohocken, PA:

C780 Standard Specification for Mortar for Unit Masonry, Vol. 04.05.
C1019 Standard Test Method for Sampling and Testing Grout, Vol. 04.04.
C1314 Standard Test Method for Compressive Strength of Masonry Prisms, Vol.04.05.

CMR Report 1998, Volume 10, No. 2, Council for Masonry Research, Herndon, VA, 1998.

Eikanas 2003, Ian K., "Behavior of Concrete Masonry Shear Walls with Varying Aspect Ratio and Flexural Reinforcement." M.S. Thesis, Department of Civil and Environmental Engineering, Washington State University, Pullman, WA, August 2003.

Hammons, M. I., Atkinson, R. H., Schuller, M. P., Tikalsky, P. J., "Masonry Research for Limit-States Design." Construction Productivity Advancement Research Program Technical Report, CPAR-SL-94-1, October 1994.

International Building Code: 2006. Country Club Hills, IL.

Masonry Standards Joint Committee: 2002, *Building Code Requirements for Masonry Structures*, ACI 530-02, American Concrete Institute, Farmington Hills, MI, ASCE-02, American Society of Civil Engineers, Reston, VA, TMS 402-02, The Masonry Society, Boulder, CO.

Masonry Standards Joint Committee: 2005, *Building Code Requirements for Masonry Structures*, ACI 530-05, American Concrete Institute, Farmington Hills, MI, ASCE-05, American Society of Civil Engineers, Reston, VA, TMS 402-052, The Masonry Society, Boulder, CO.

National Concrete Masonry Association: 2004, MR26. "Effects of Confinement Reinforcement on Bar Splice Performance." July 2004.

National Concrete Masonry Association: 2005, MR27. "Effects of Confinement Reinforcement on Bar Splice Performance – Phase II." November 2005.

National Concrete Masonry Association: 2007, MR32. "Effects of Confinement Reinforcement on Bar Splice Performance – Phase III." October 2007.

Snook 2005, Matthew K., "Effects of Confinement Reinforcement on the Performance of Masonry Shear Walls." M.S. Thesis, Department of Civil and Environmental Engineering, Washington State University, Pullman, WA, August 2005.

Soric 1987, Z., Tulin, L. G., “Bond Stress and Slip in Masonry Reinforced with Spliced Reinforcement.” TMS Journal, The Masonry Society, Vol. 6, No. 1.

Thompson, Jason J., “Behavior and Design of Tension Lap Splices in Reinforced Concrete Masonry.” M.S. Thesis, Department of Civil and Environmental Engineering, Washington State University, Pullman, WA, August 1997.

XTRACT, Version 3.0.7 *Imbsen & Associated Inc. Engineering Consultants.* 2007. *www.imbsen.com*

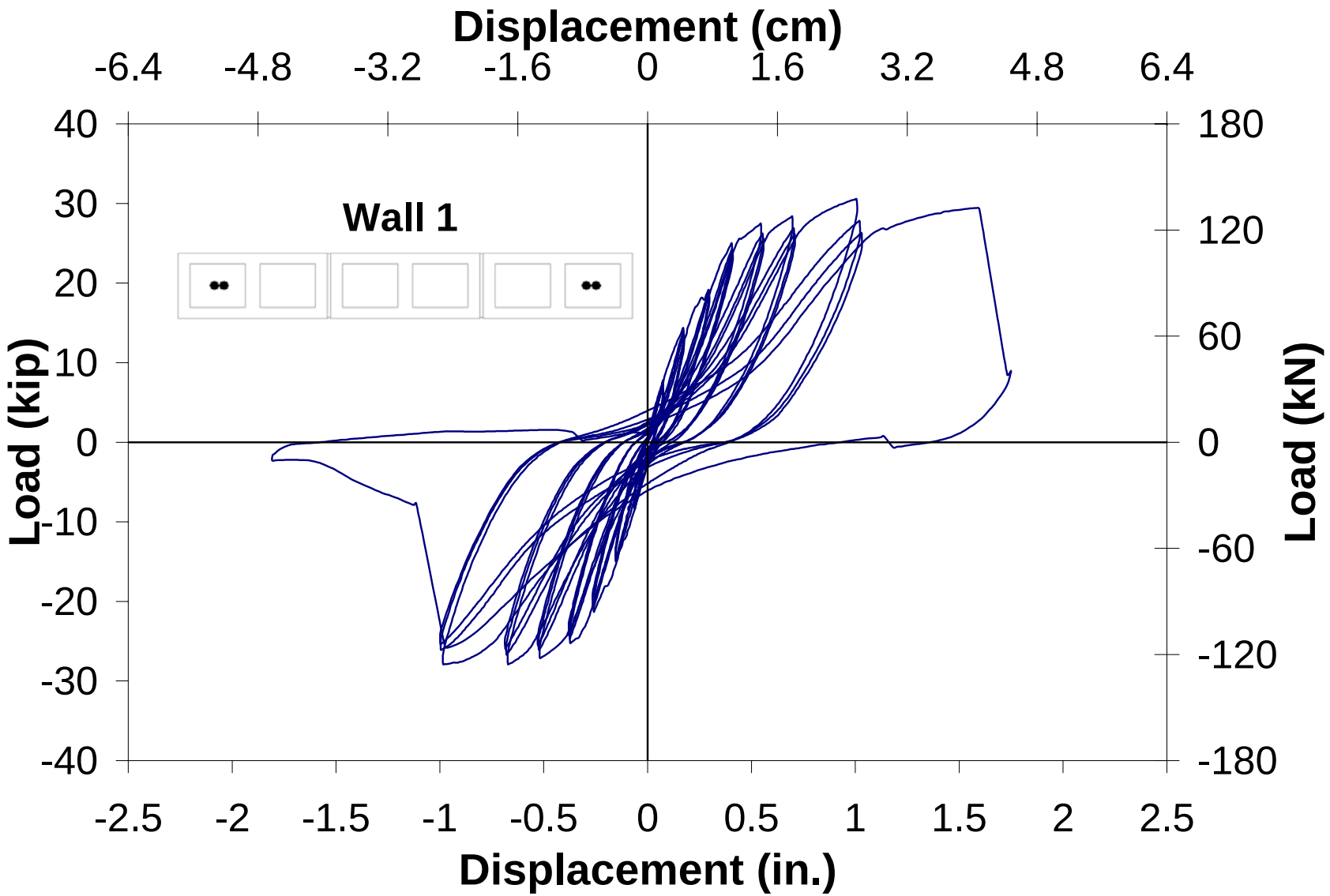
Displacement (cm)
-6.4
-4.8
-3.2
-1.6
0
1.6
3.2
4.8
6.4
Wall 1
Load (kip)
40
30
20
10
0
-10
-20
-30
-40
Load (kN)
180
120
60
0
-60
-120
-180
-2.5
-2
-1.5
-1
-0.5
0
0.5
1
1.5
2
2.5
Displacement (in.)

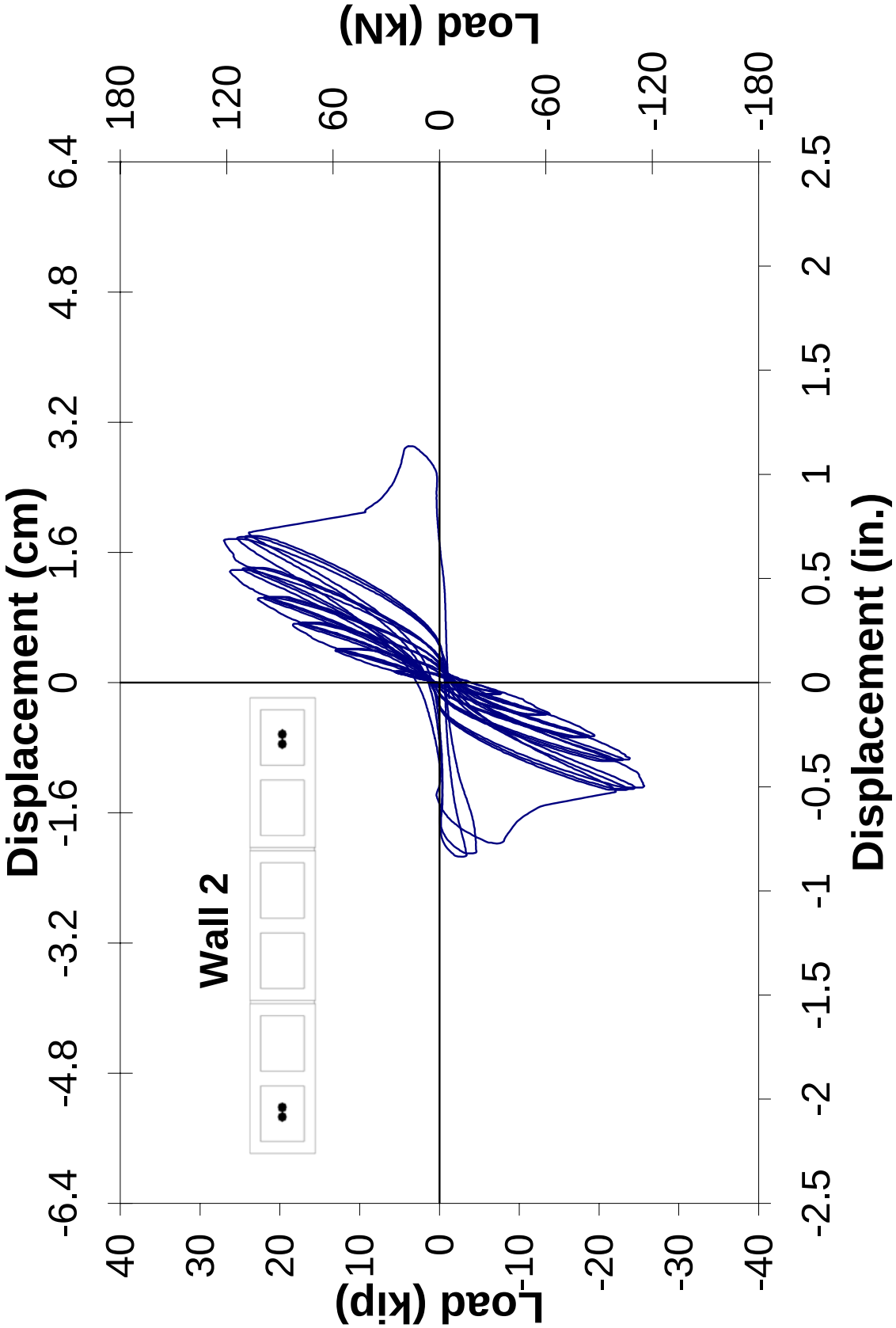
Wall 2
Displacement (cm)
-6.4
-4.8
-3.2
-1.6
0
1.6
3.2
4.8
6.4
Load (kip)
40
30
20
10
0
-10
-20
-30
-40
Displacement (in.)
-2.5
-2
-1.5
-1
-0.5
0
0.5
1
1.5
2
2.5
Load (kN)
180
120
60
0
-60
-120
-180

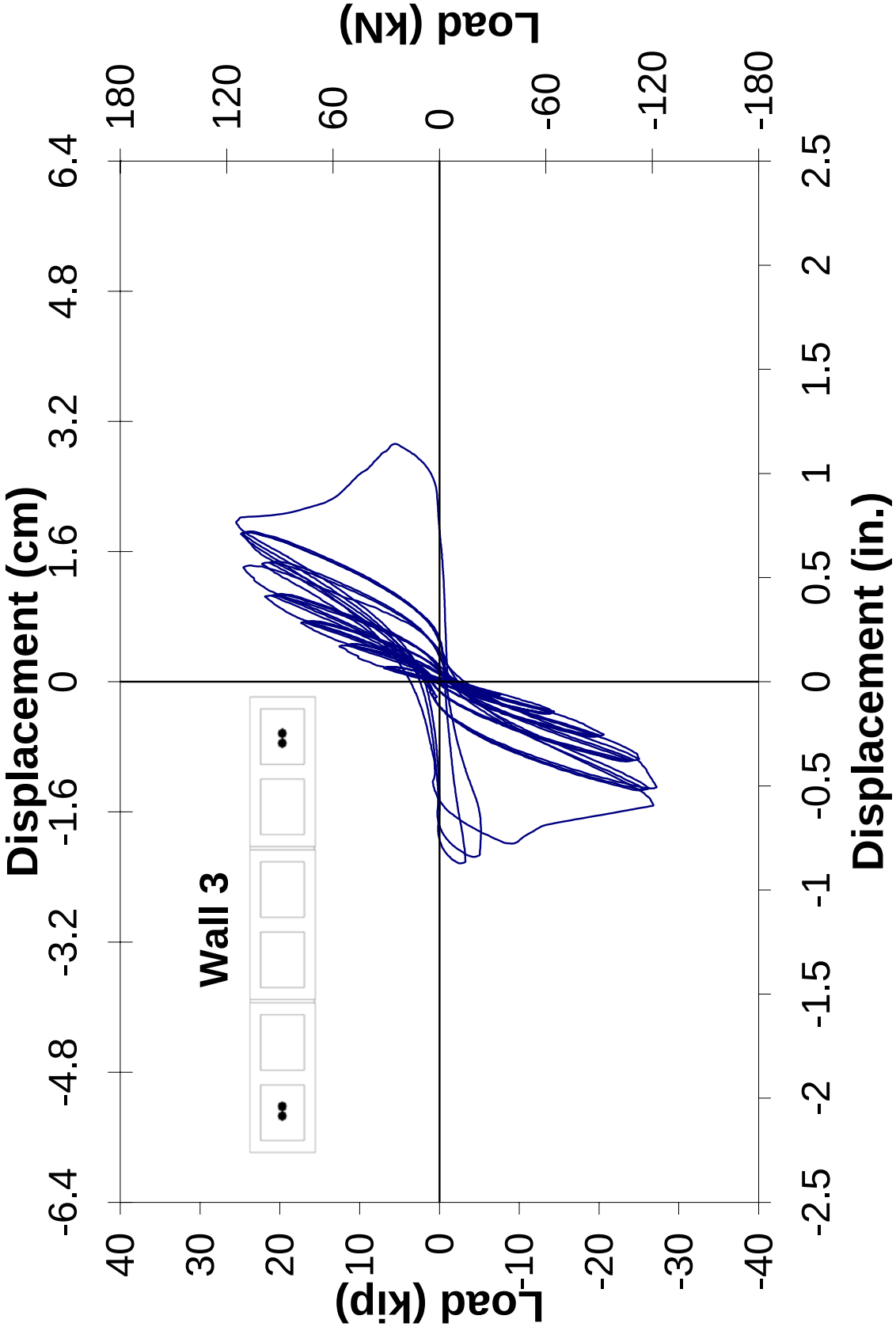
Wall 3
Displacement (cm)
-6.4
-4.8
-3.2
-1.6
0
1.6
3.2
4.8
6.4
Load (kip)
40
30
20
10
0
-10
-20
-30
-40
Displacement (in.)
-2.5
-2
-1.5
-1
-0.5
0
0.5
1
1.5
2
2.5
Load (kN)
180
120
60
0
-60
-120
-180

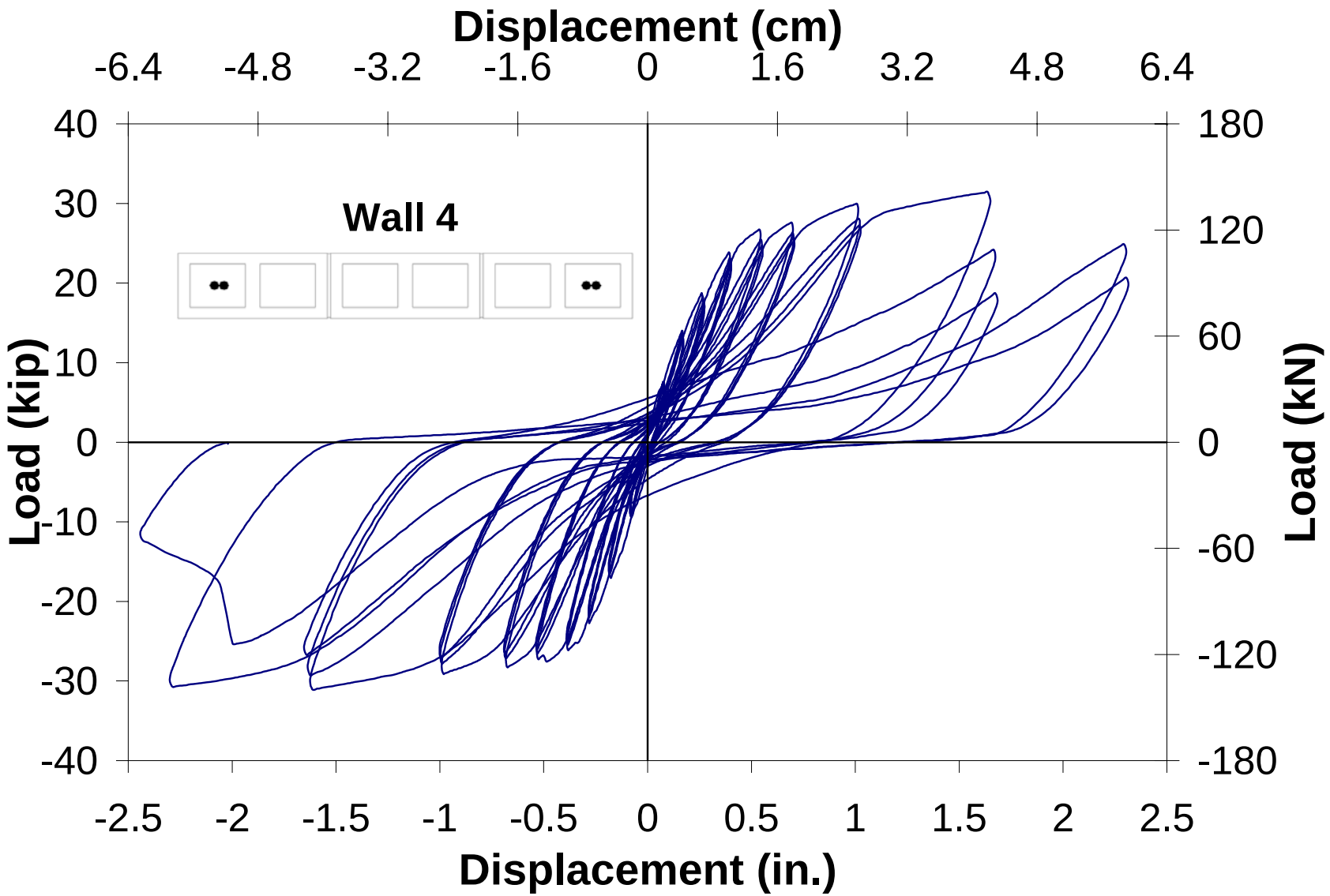
Displacement (cm)
-6.4
-4.8
-3.2
-1.6
0
1.6
3.2
4.8
6.4
Wall 4
Load (kip)
40
30
20
10
0
-10
-20
-30
-40
Load (kN)
180
120
60
0
-60
-120
-180
-2.5
-2
-1.5
-1
-0.5
0
0.5
1
1.5
2
2.5
Displacement (in.)

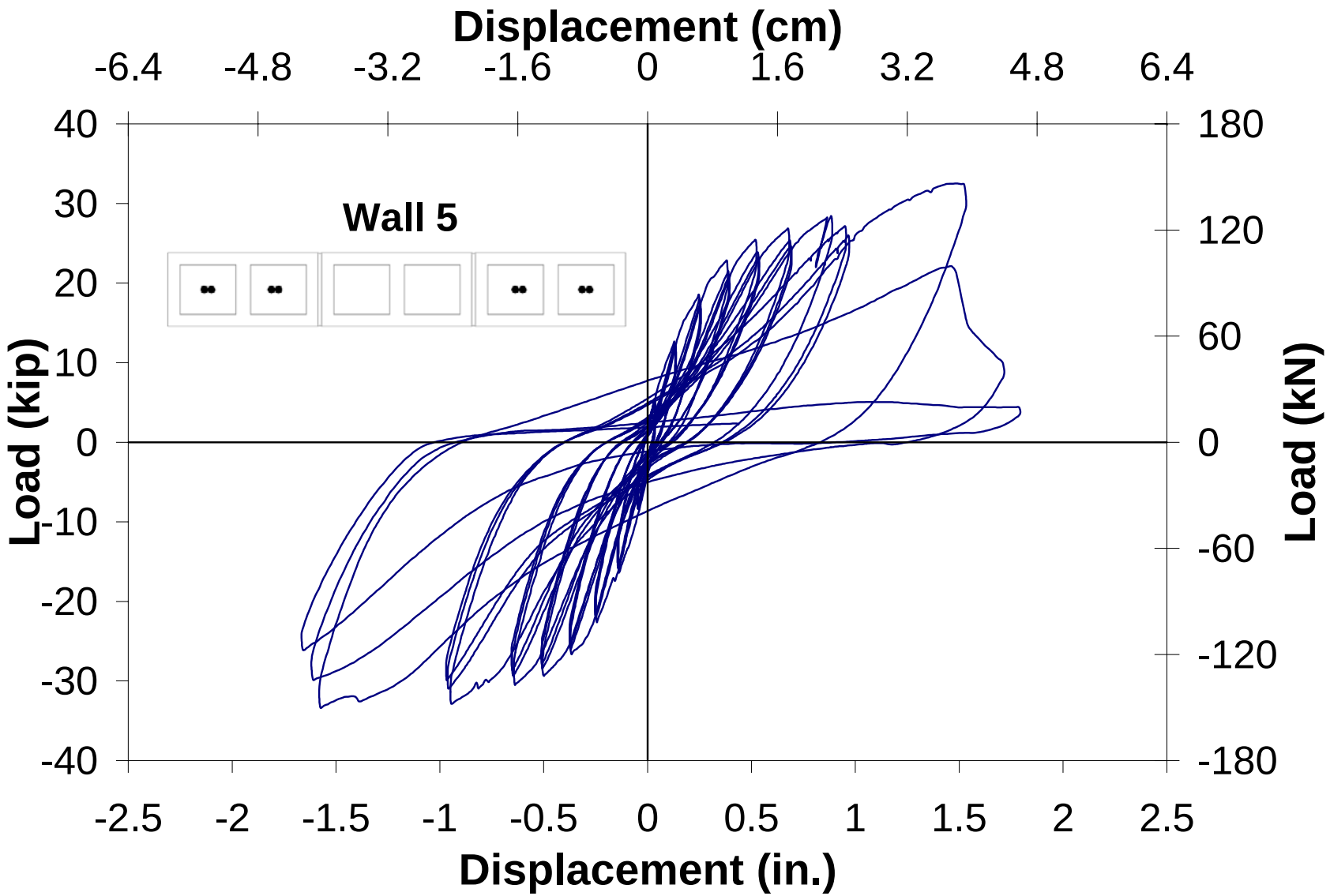
Displacement (cm)
-6.4
-4.8
-3.2
-1.6
0
1.6
3.2
4.8
6.4
Wall 5
Load (kip)
40
30
20
10
0
-10
-20
-30
-40
Load (kN)
180
120
60
0
-60
-120
-180
-2.5
-2
-1.5
-1
-0.5
0
0.5
1
1.5
2
2.5
Displacement (in.)

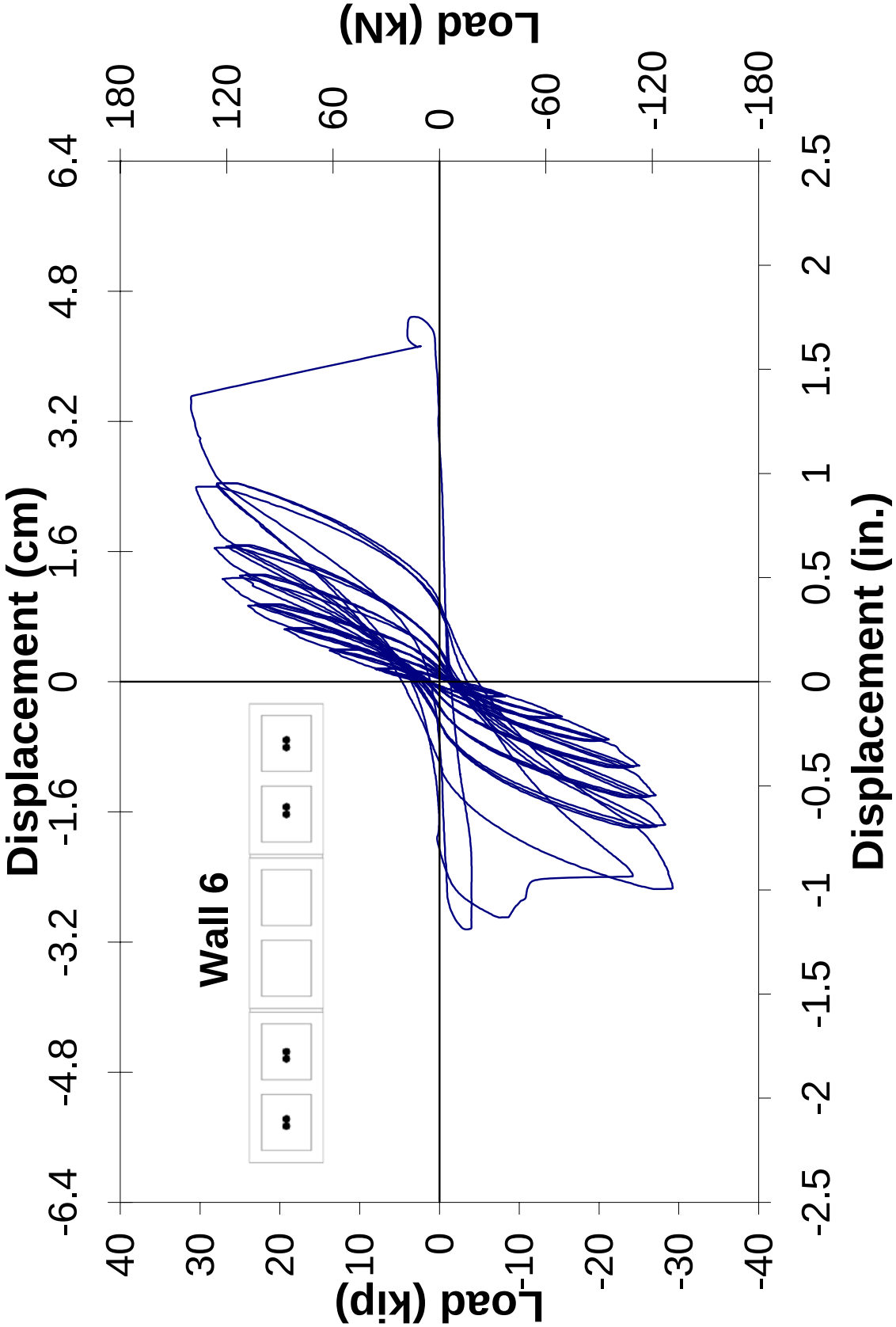
Wall 6
Displacement (cm)
-6.4
-4.8
-3.2
-1.6
0
1.6
3.2
4.8
6.4
Load (kip)
40
30
20
10
0
-10
-20
-30
-40
Displacement (in.)
-2.5
-2
-1.5
-1
-0.5
0
0.5
1
1.5
2
2.5
Load (kN)
180
120
60
0
-60
-120
-180

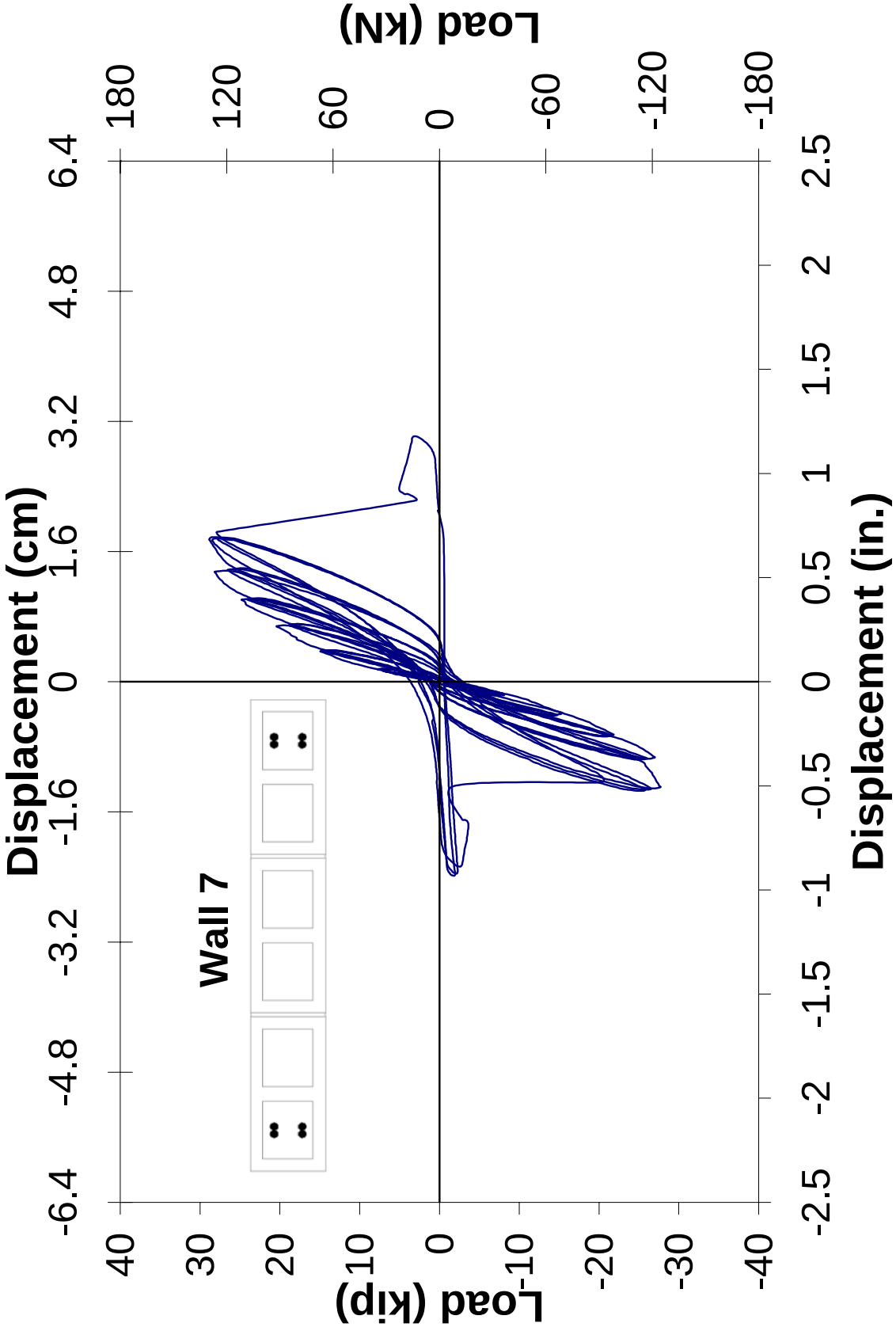
Wall 7
Displacement (cm)
-6.4
-4.8
-3.2
-1.6
0
1.6
3.2
4.8
6.4
Load (kip)
40
30
20
10
0
-10
-20
-30
-40
Displacement (in.)
-2.5
-2
-1.5
-1
-0.5
0
0.5
1
1.5
2
2.5
Load (kN)
180
120
60
0
-60
-120
-180

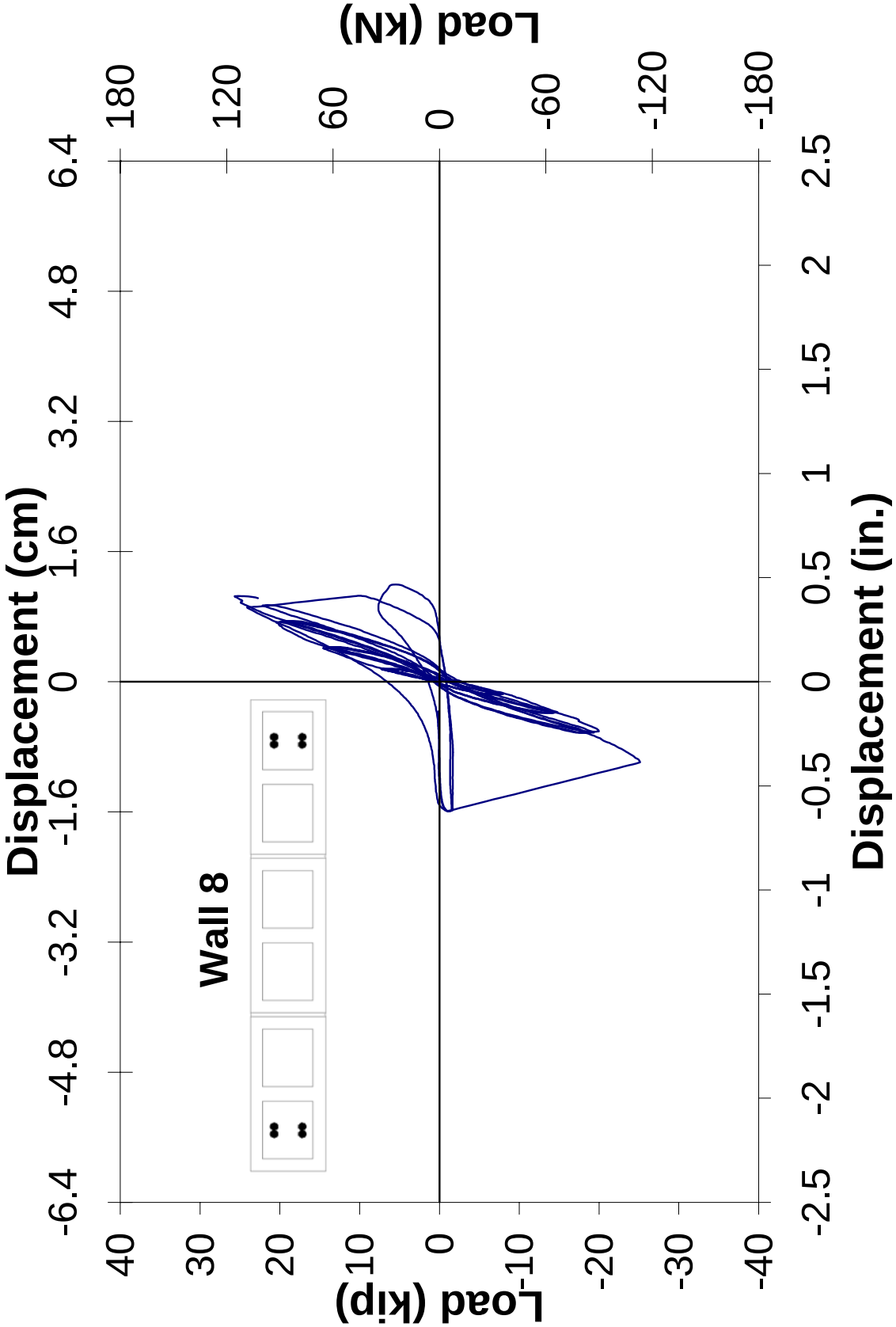
Wall 8
Displacement (cm)
-6.4
-4.8
-3.2
-1.6
0
1.6
3.2
4.8
6.4
Load (kip)
40
30
20
10
0
-10
-20
-30
-40
Displacement (in.)
-2.5
-2
-1.5
-1
-0.5
0
0.5
1
1.5
2
2.5
Load (kN)
180
120
60
0
-60
-120
-180

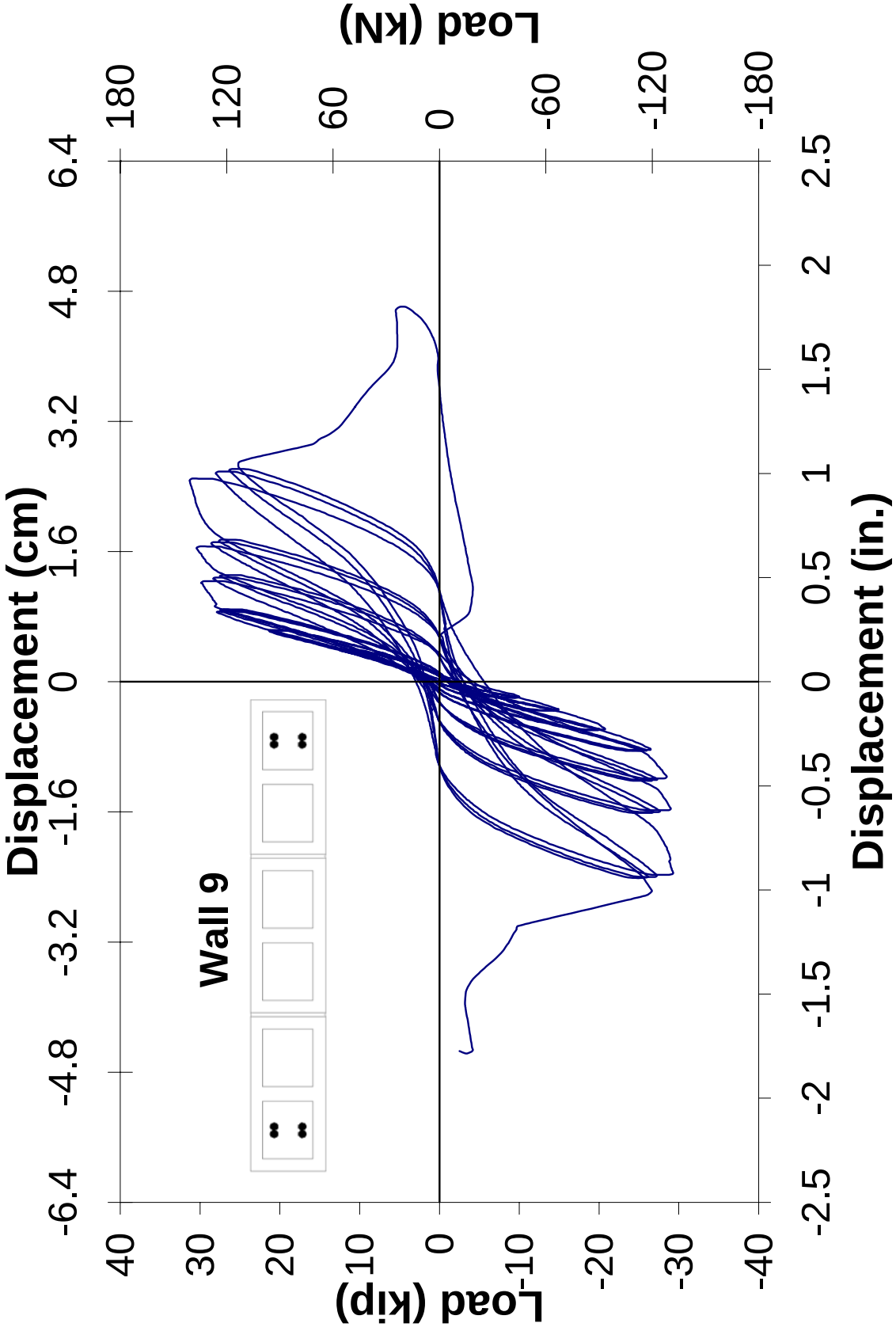
Wall 9
Displacement (cm)
-6.4
-4.8
-3.2
-1.6
0
1.6
3.2
4.8
6.4
Load (kip)
40
30
20
10
0
-10
-20
-30
-40
Displacement (in.)
-2.5
-2
-1.5
-1
-0.5
0
0.5
1
1.5
2
2.5
Load (kN)
180
120
60
0
-60
-120
-180